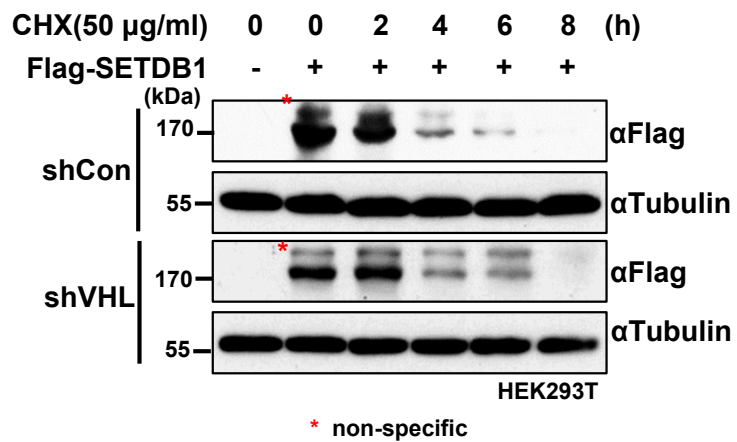
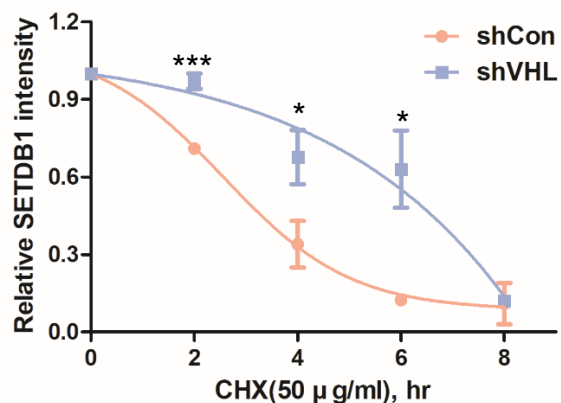


Fig S1.

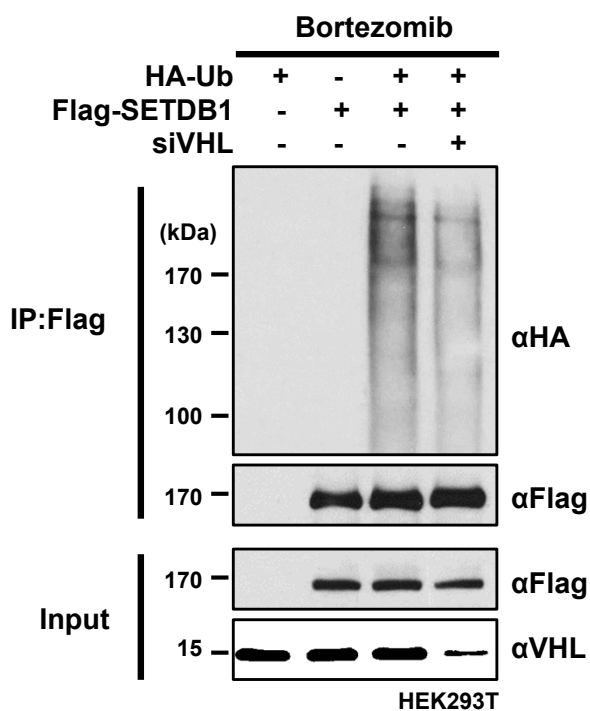
A



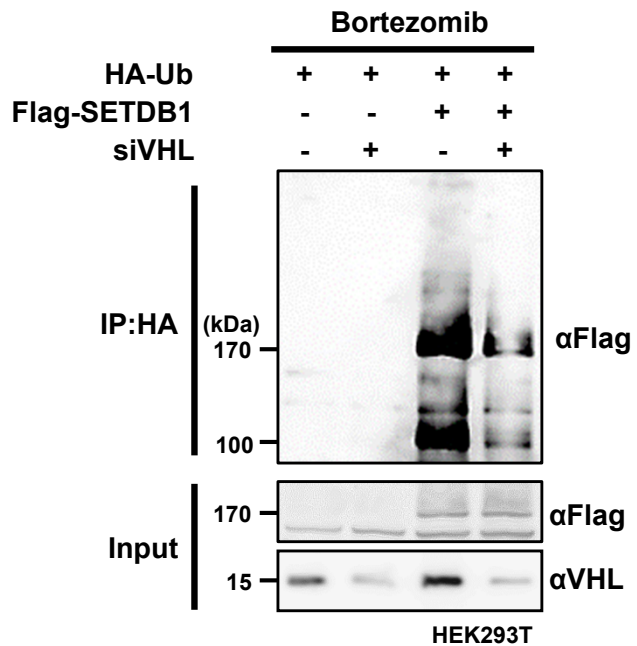
B



C



D



E

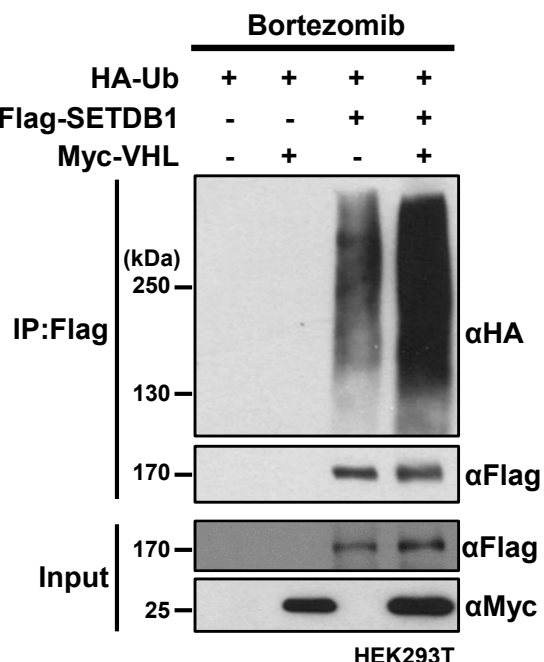
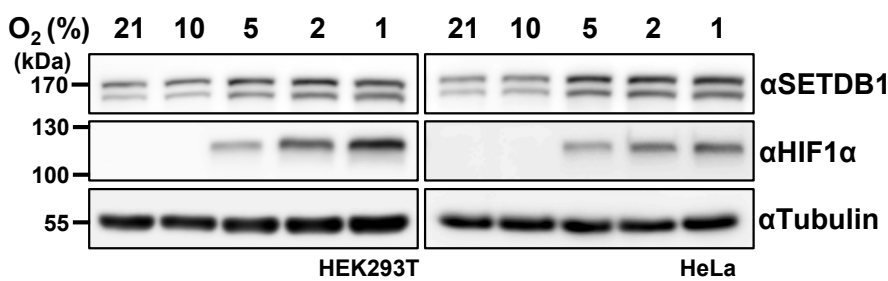
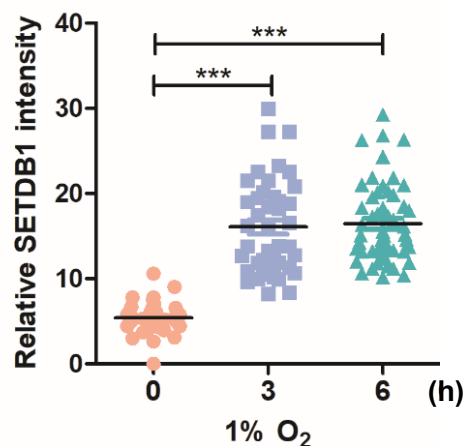


Fig S2.

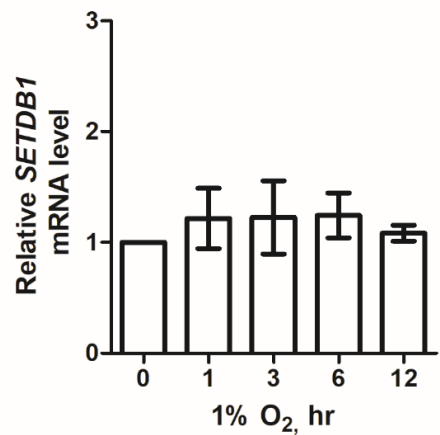
A



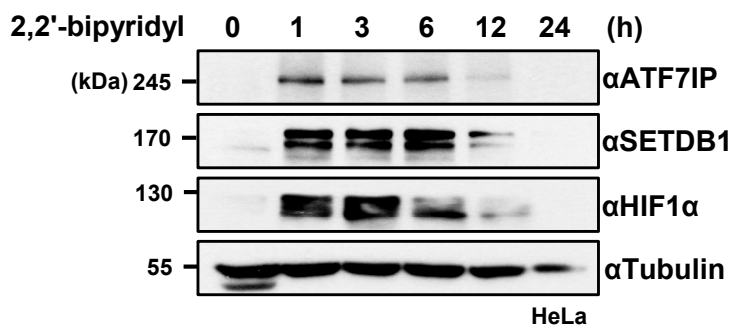
B



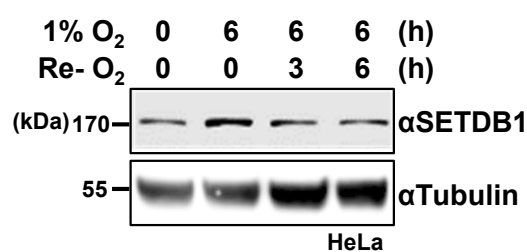
C



D



E



F

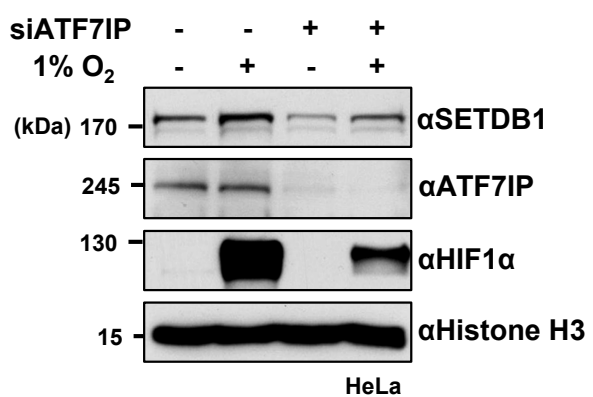


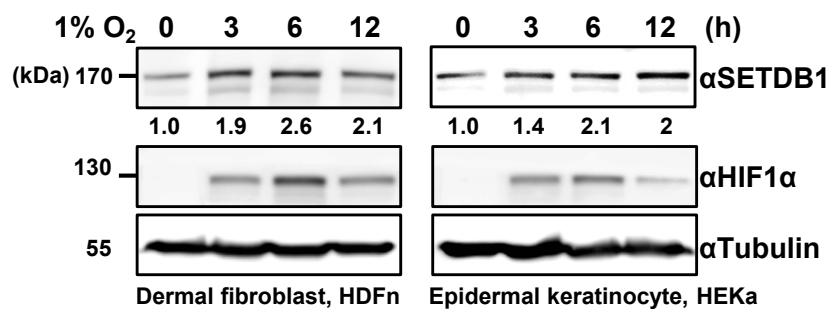
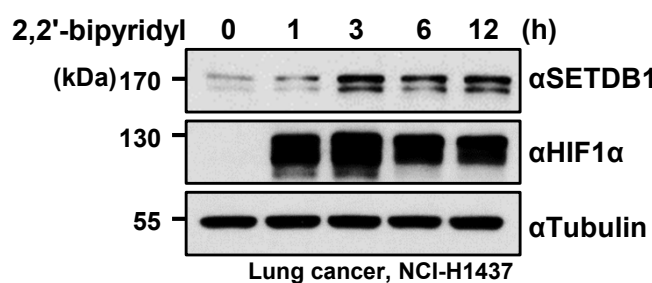
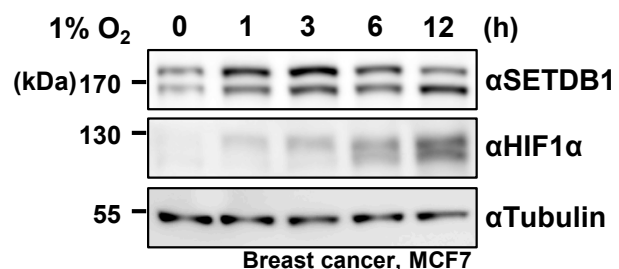
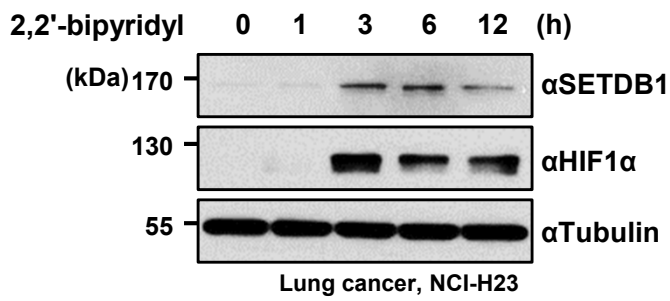
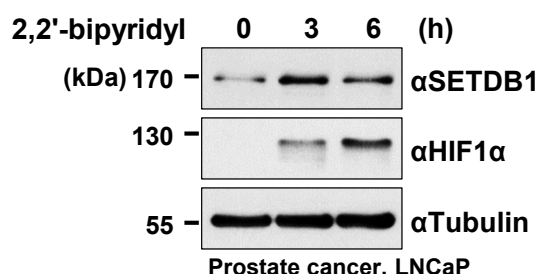
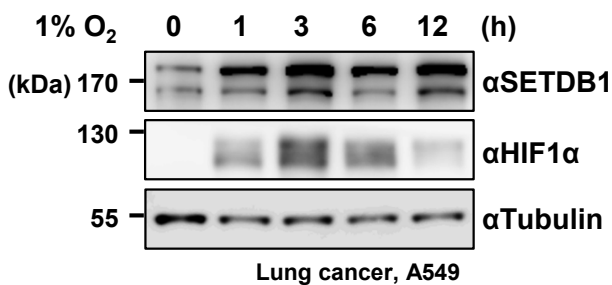
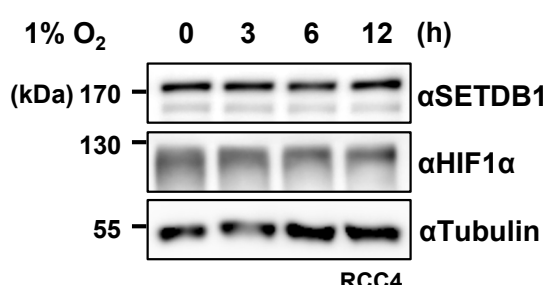
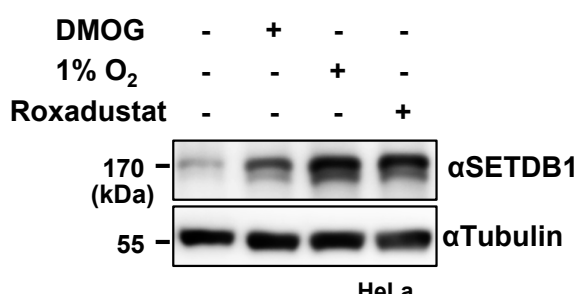
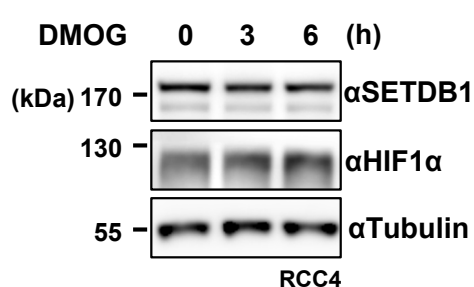
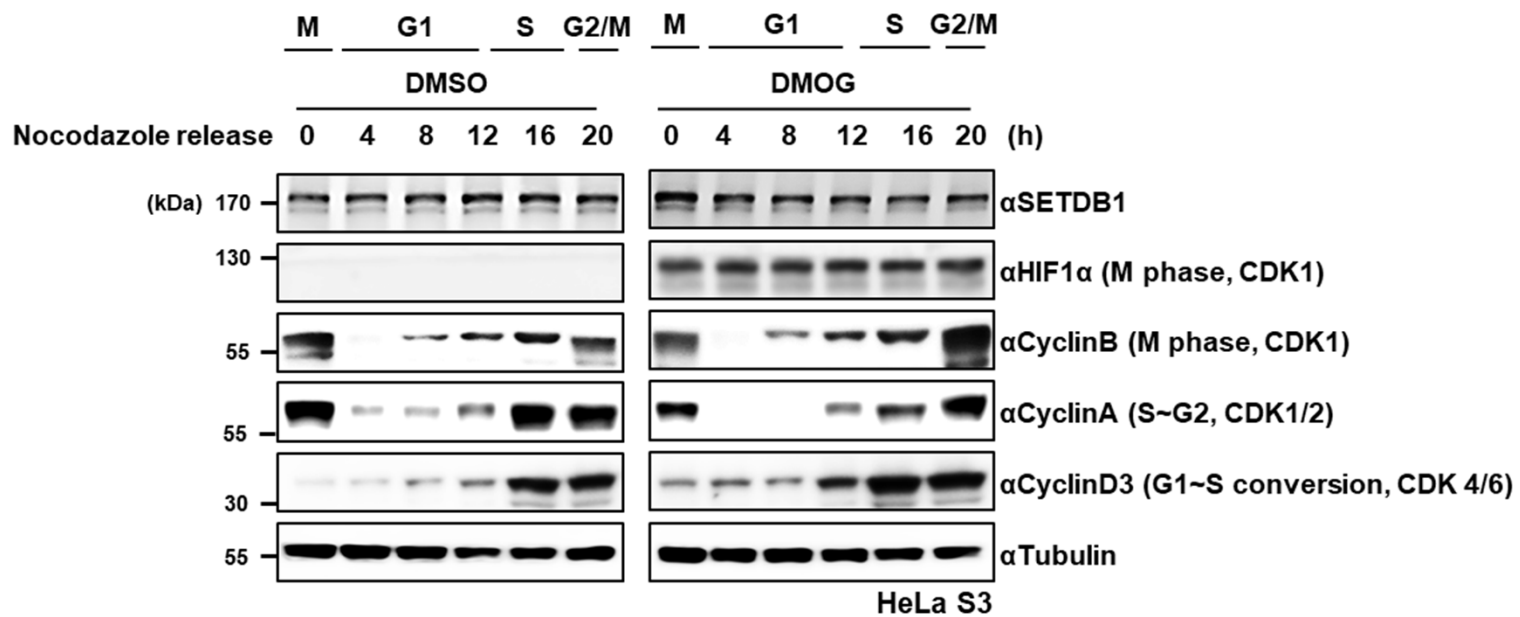
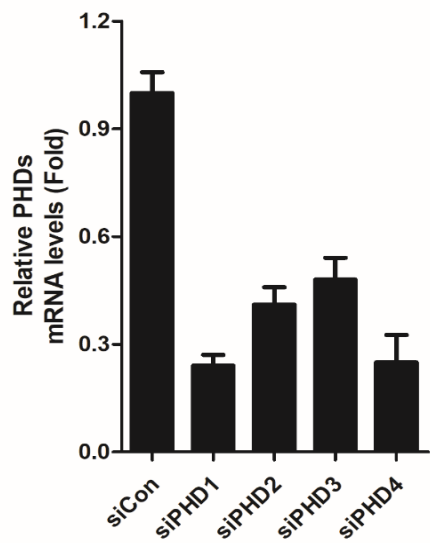
Fig S3.**A****B****C****D****E****F****G****H****I**

Fig S3.

J



K



L

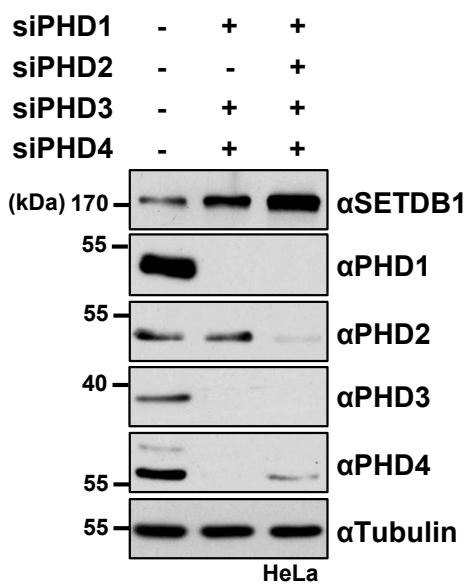


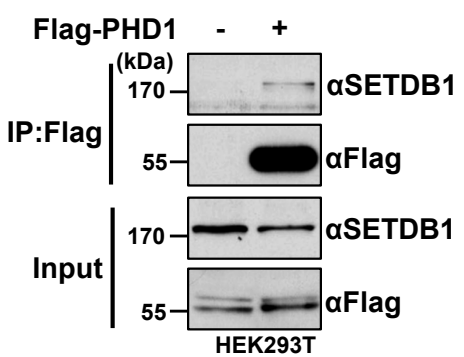
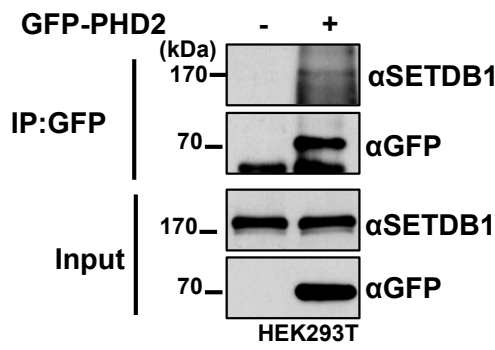
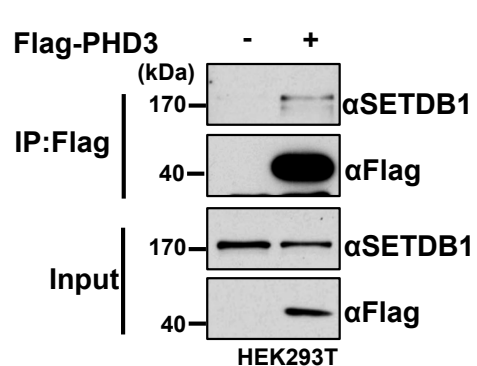
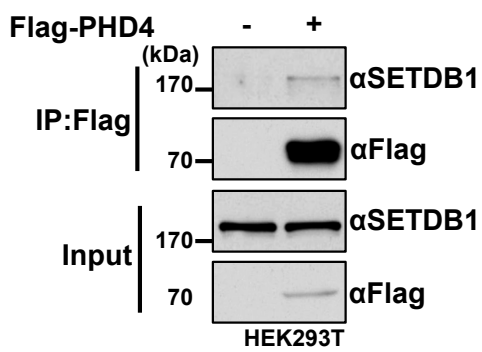
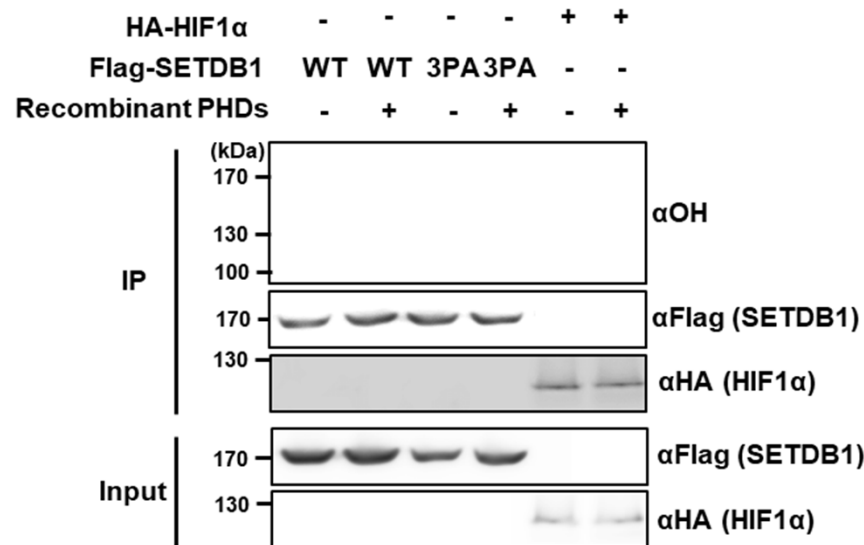
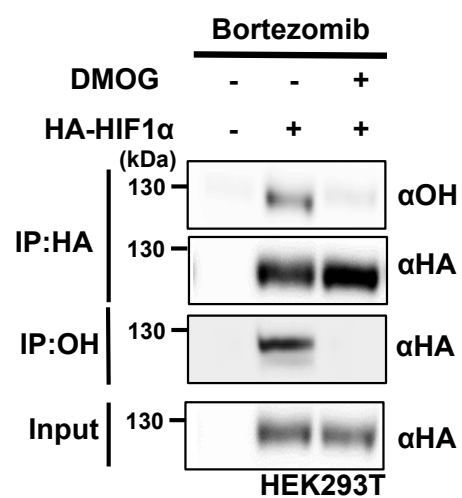
Fig S4.**A****B****C****D**

Fig S5.

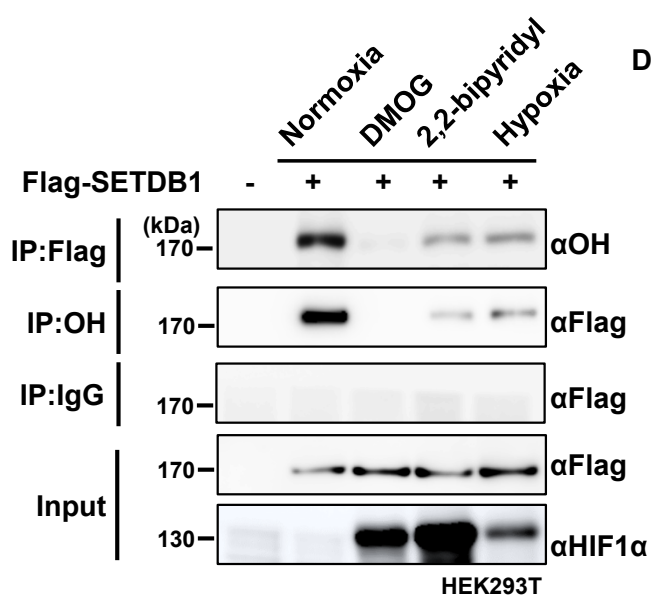
A



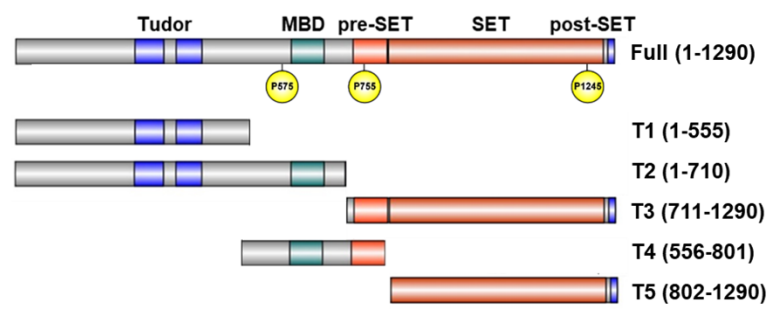
B



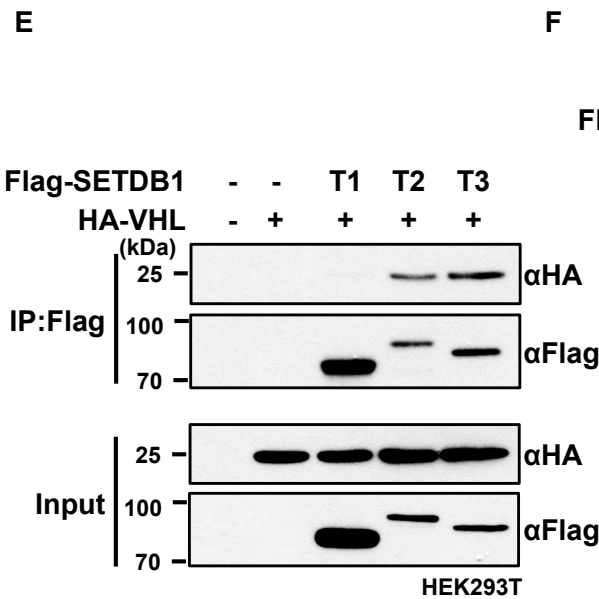
C



D



E



F

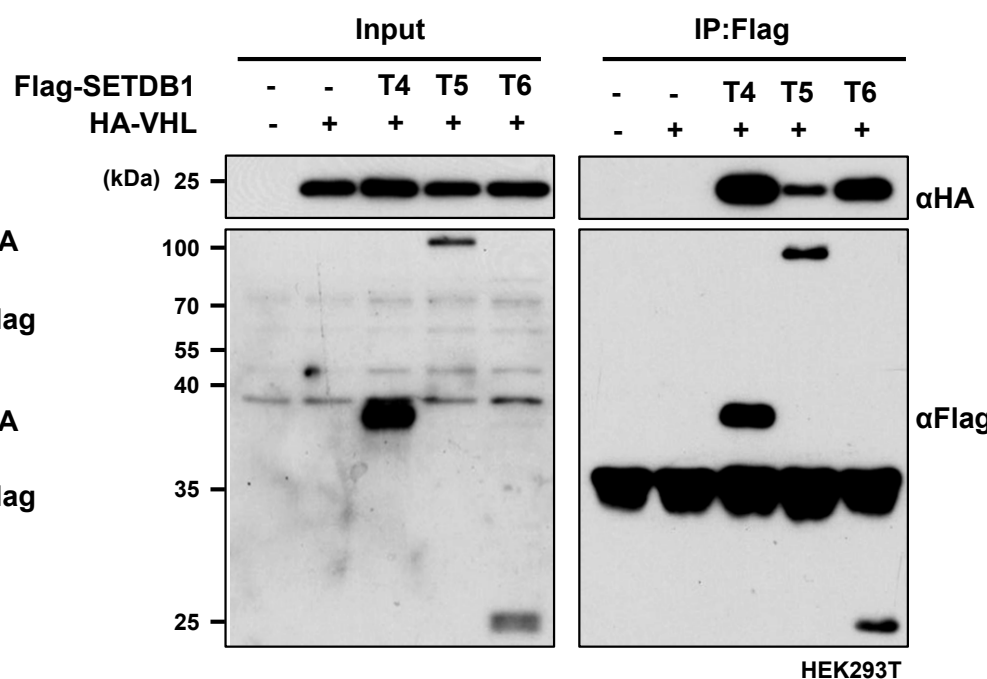
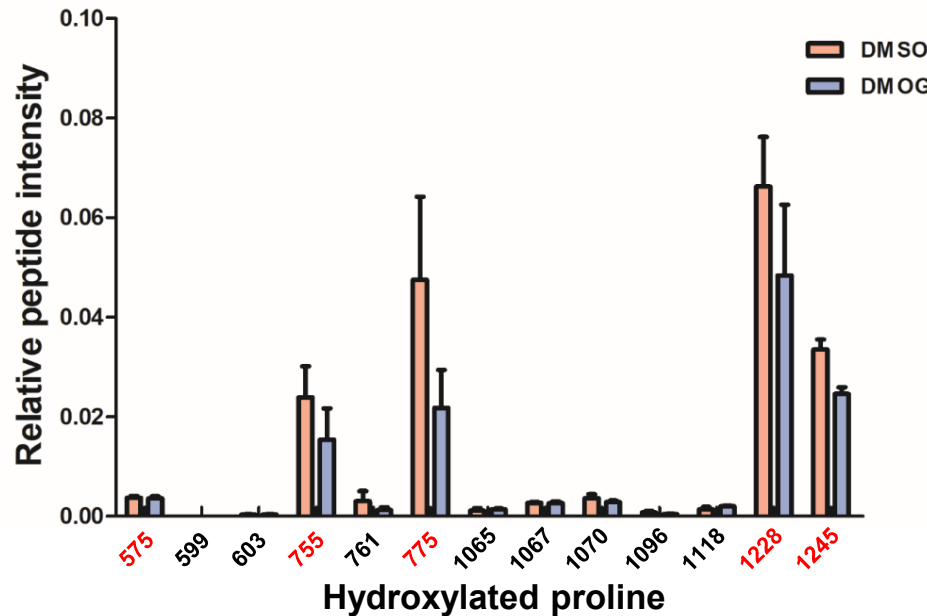


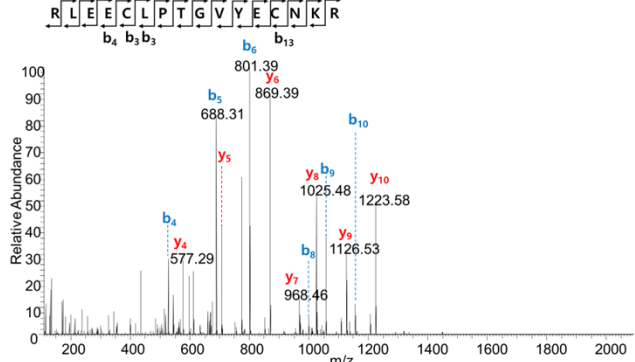
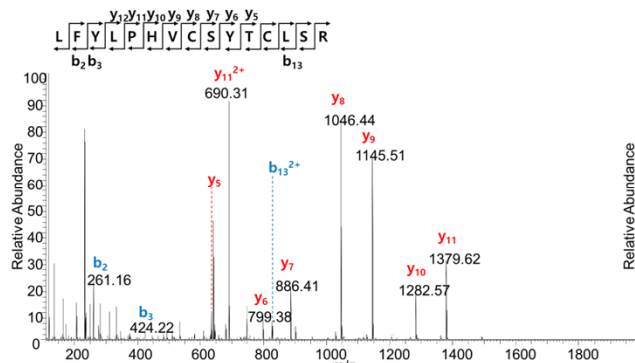
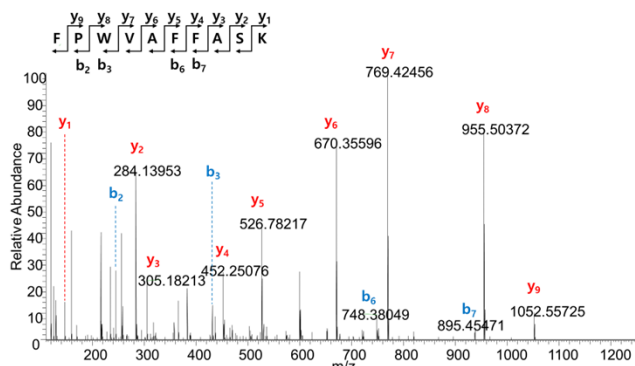
Fig S5.

G



H

Non-hydroxylated peptide



Hydroxylated peptide

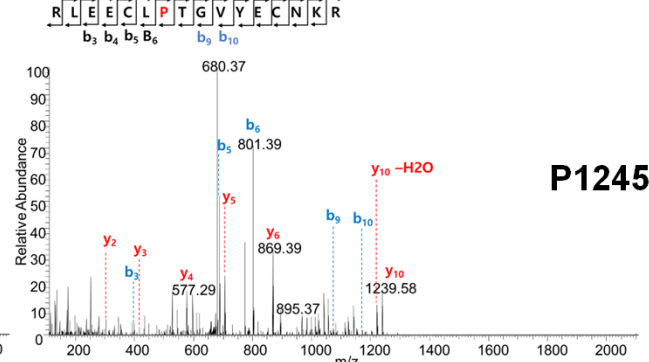
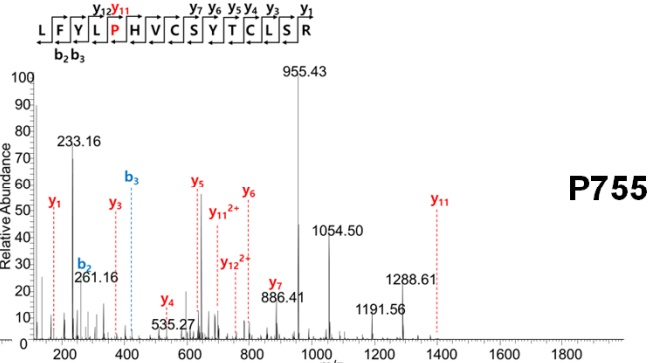
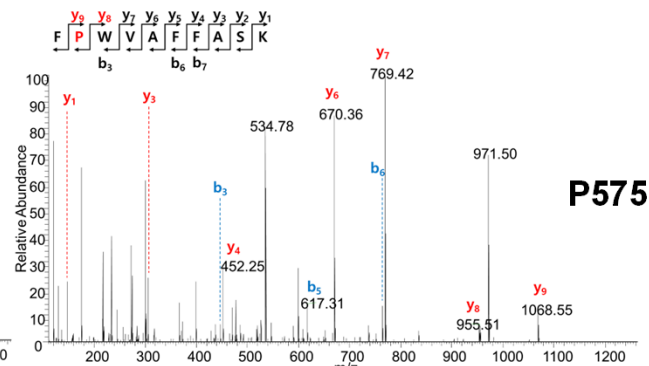
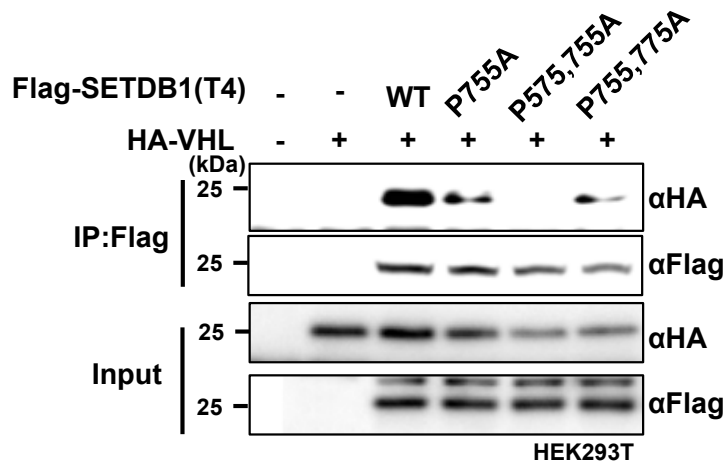
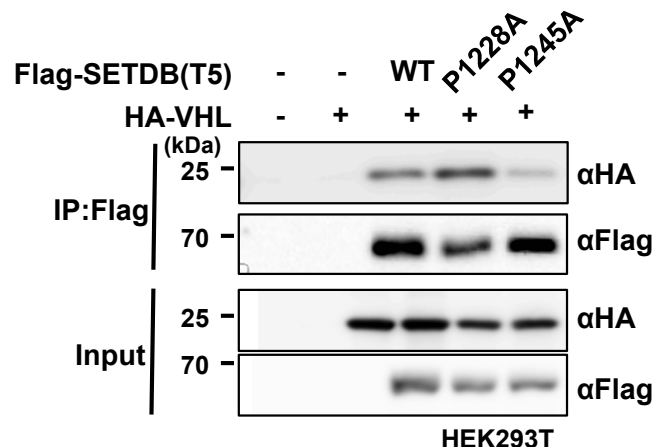


Fig S5.

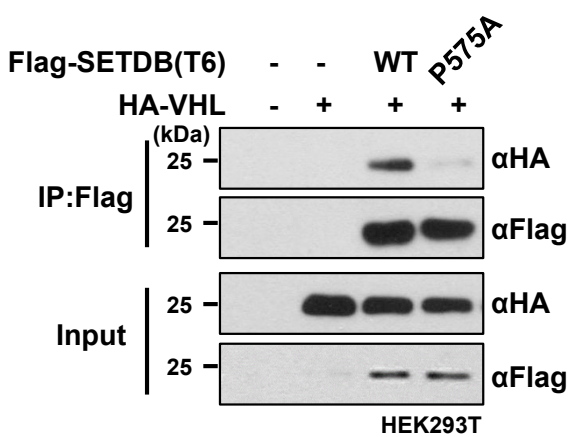
I



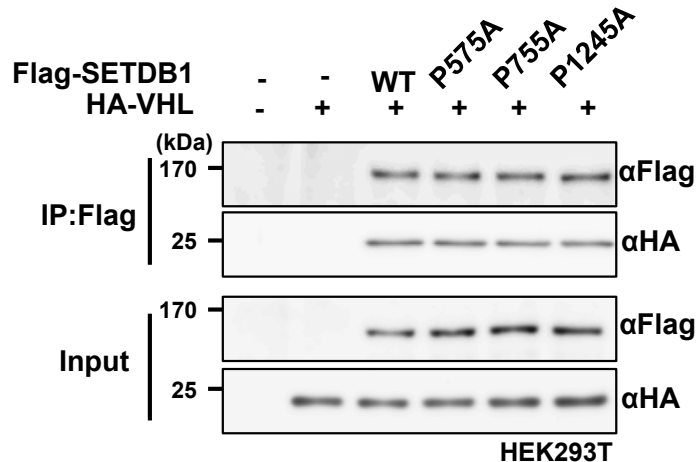
J



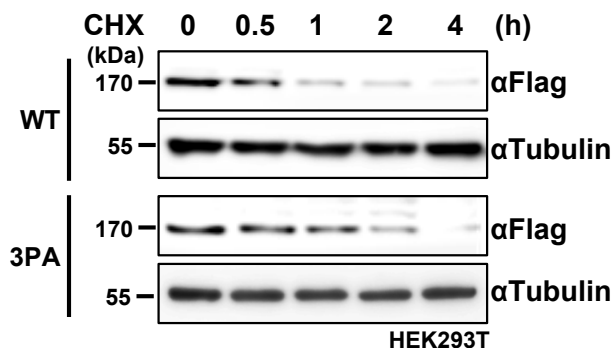
K



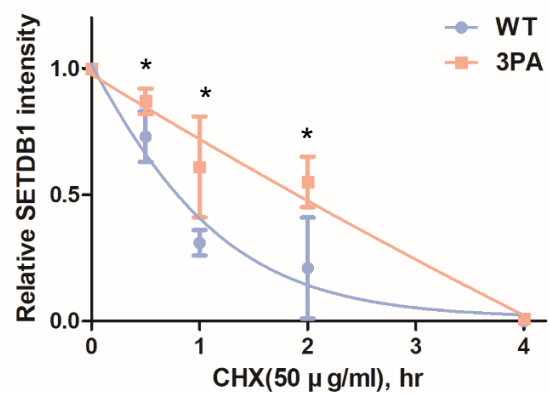
L



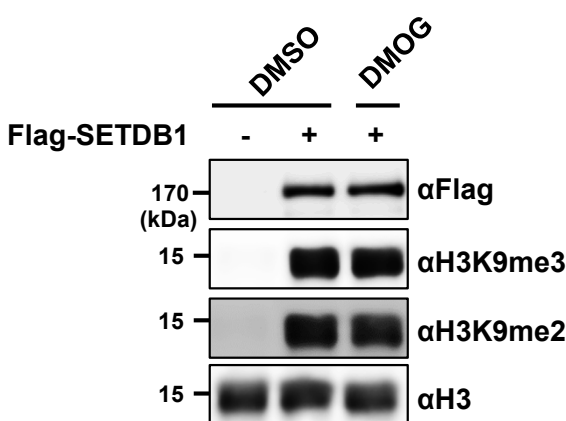
M



N



O



P

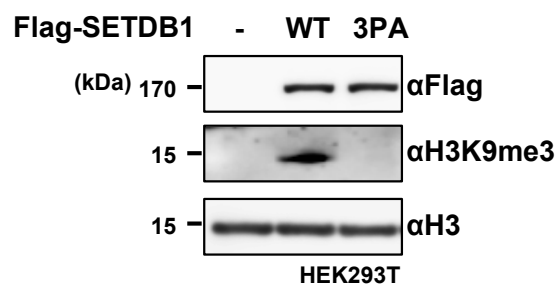
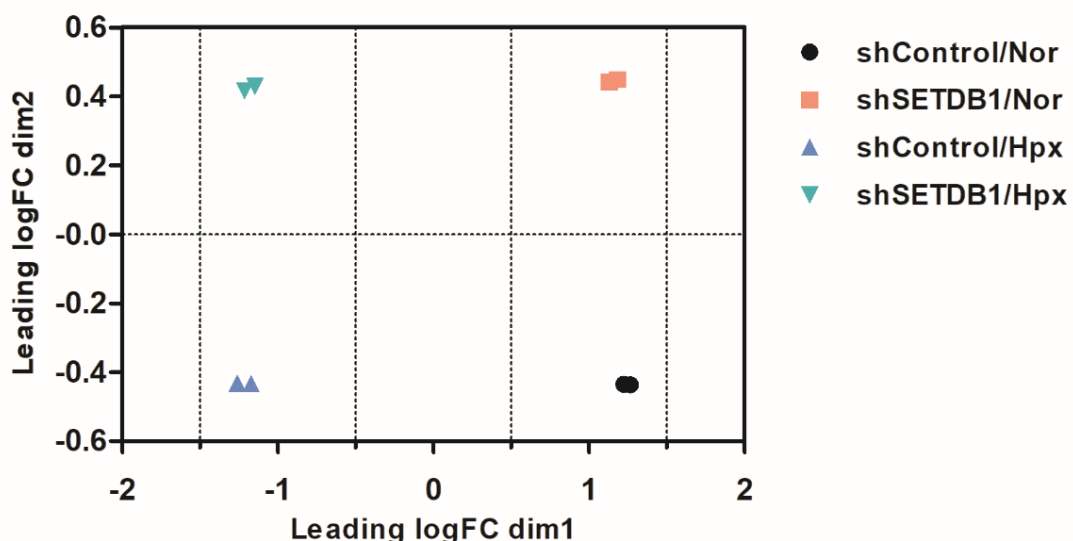
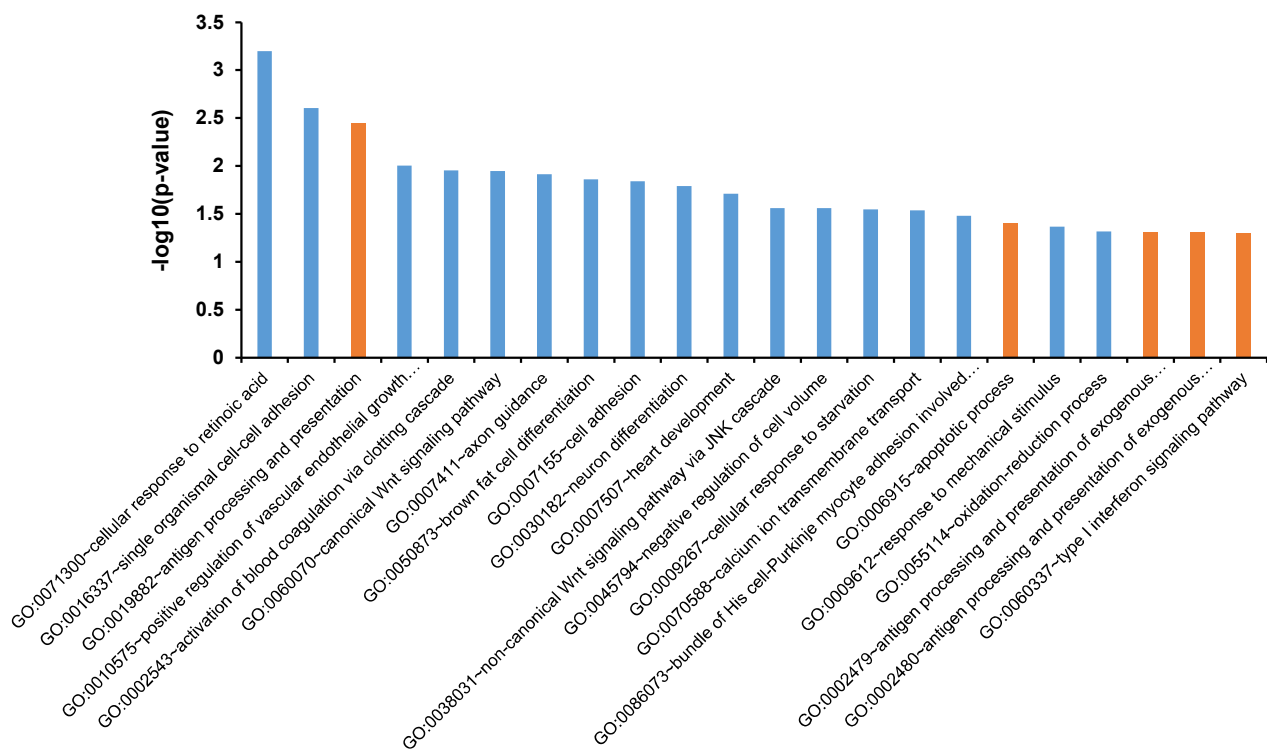


Fig S6.

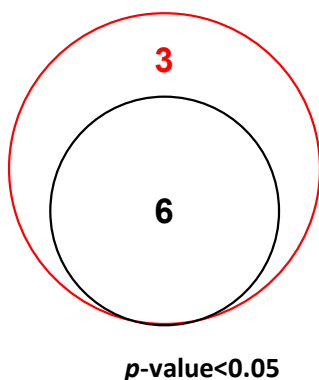
A



B



C



shSETDB1/Hpx vs shSETDB1/Nor

UV response down, NES=2.09, p=0.04

Inflammatory response, NES=2.07, p=0.04

WNT beta catenin signaling, NES=1.85, p=0.04

shControl/Hpx vs shControl/Nor

Hypoxia, NES=2.21, p=0.00

Glycolysis, NES=2.02, p=0.00

Myogenesis, NES=1.53, p=0.00

TNFA signaling via NFKB, NES=1.43, p=0.00

Epithelial mesenchymal transition, NES=1.72, p=0.00

KRAS signaling up, NES=1.54, p=0.00

p-value<0.05

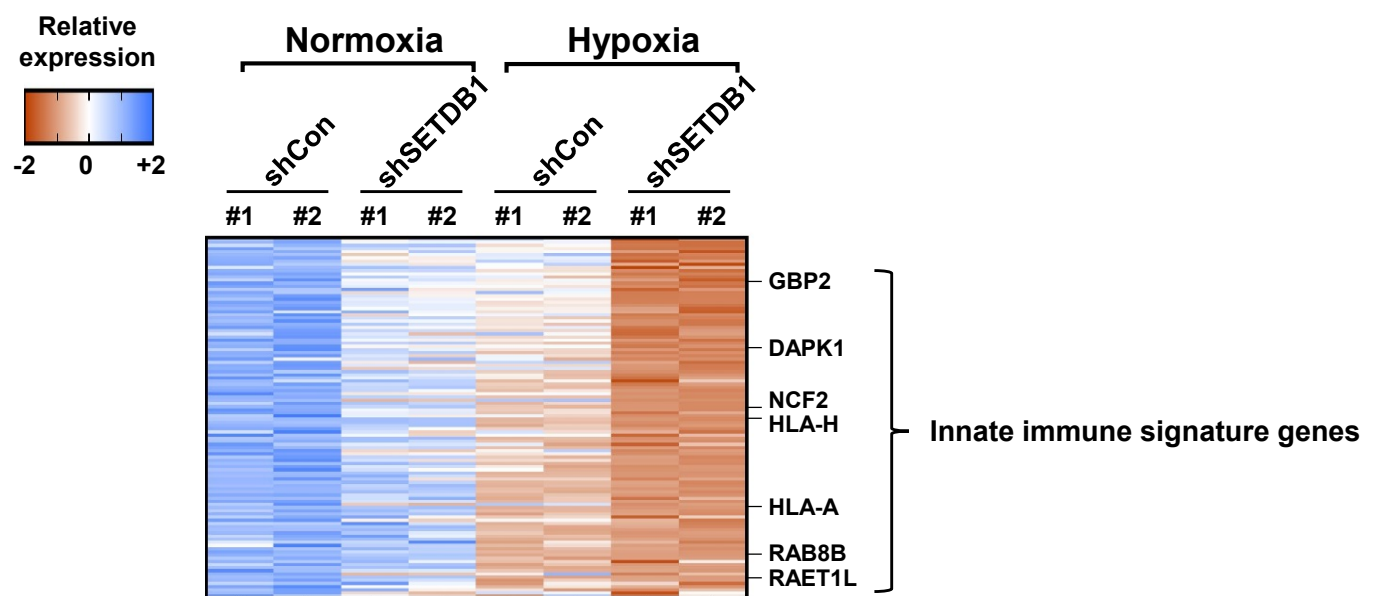
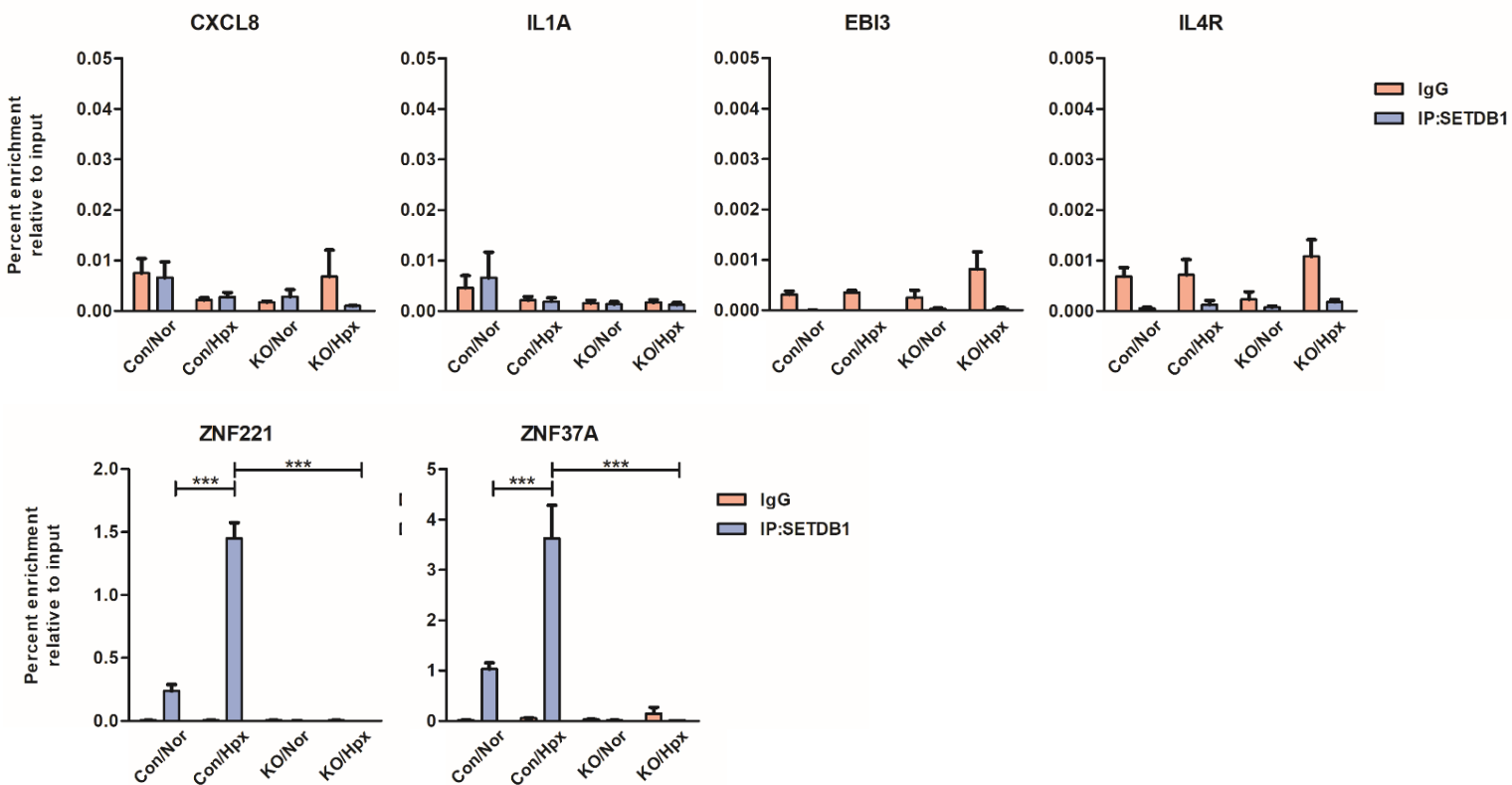
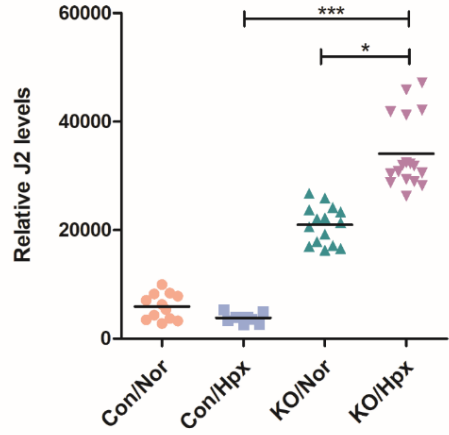
Fig S6.**D**

Fig S7.

A



B



C

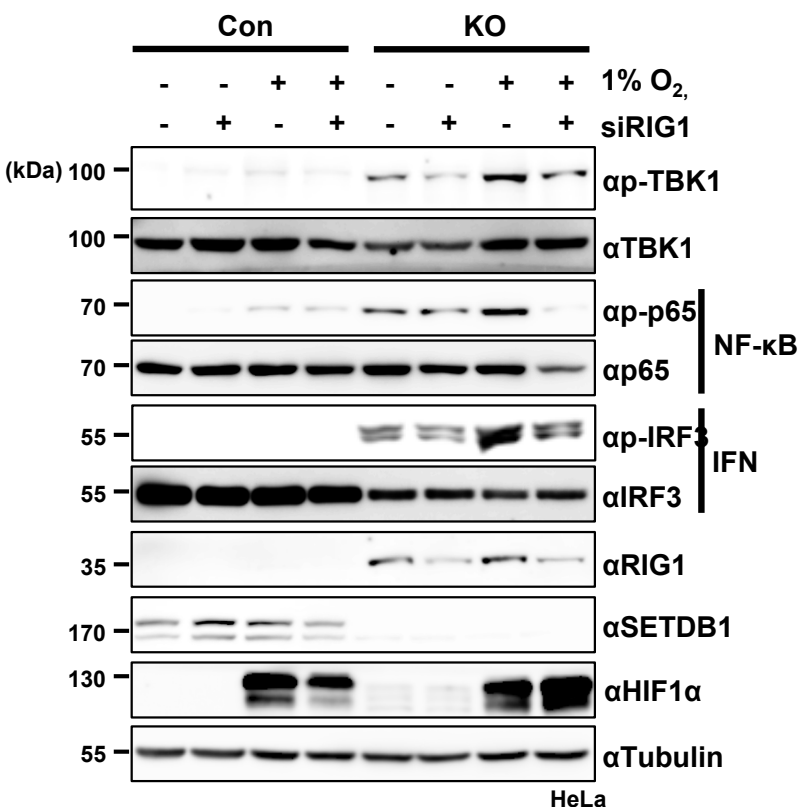
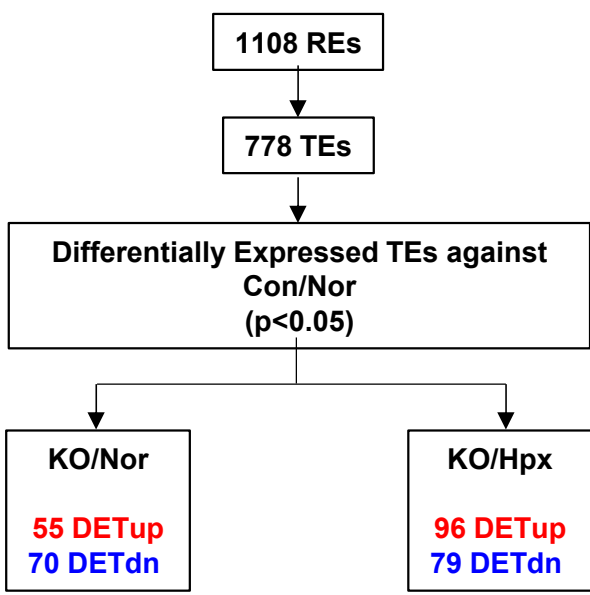
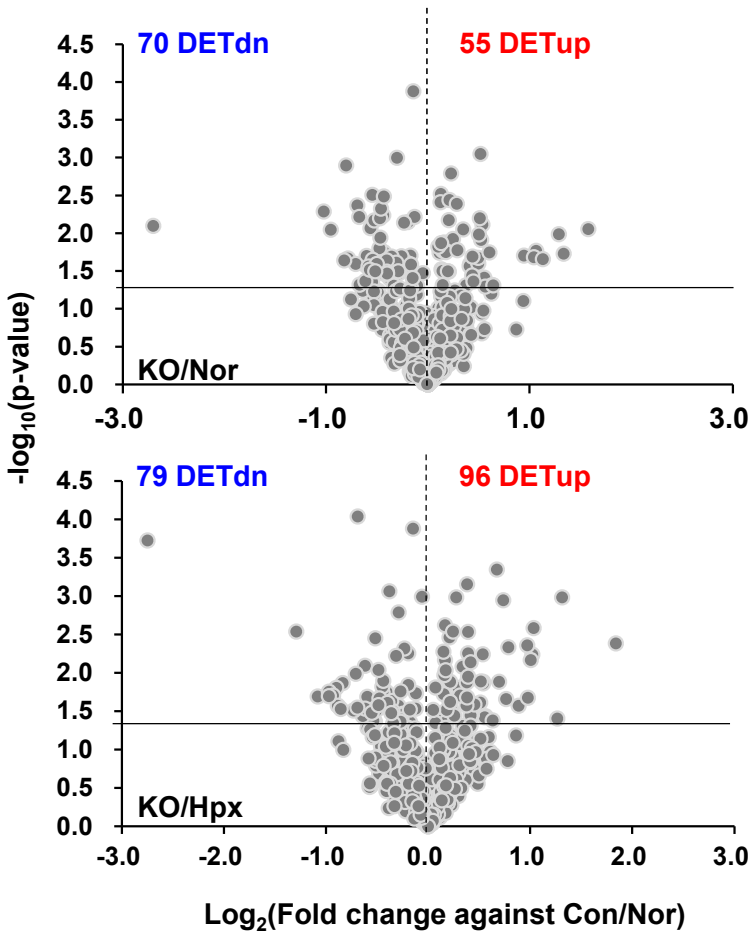


Fig S7.

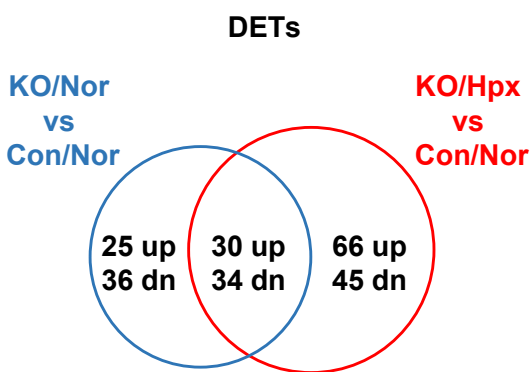
D



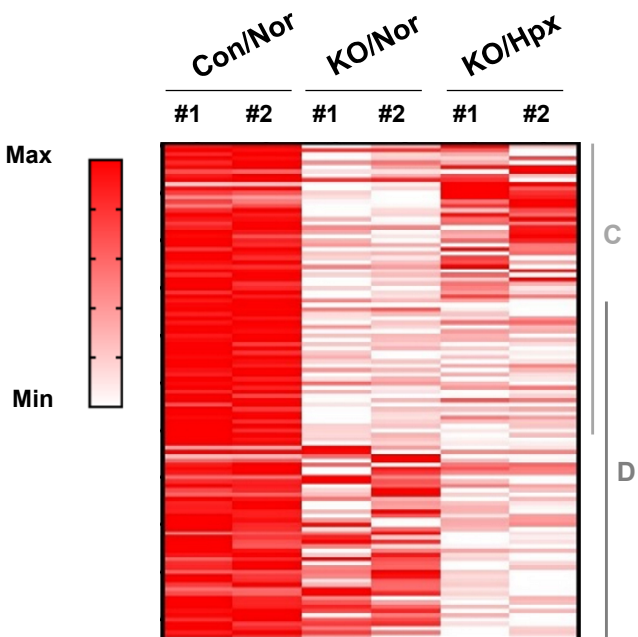
E



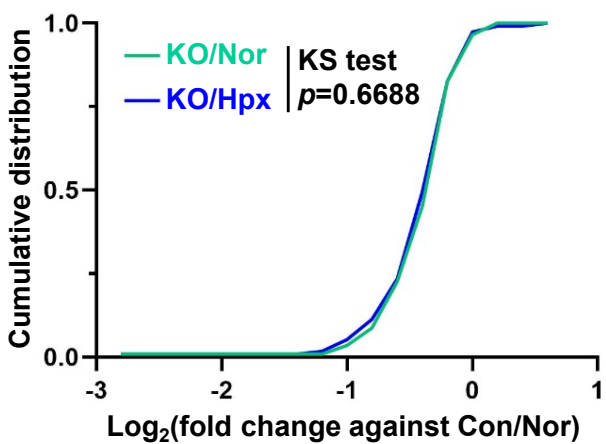
F



G



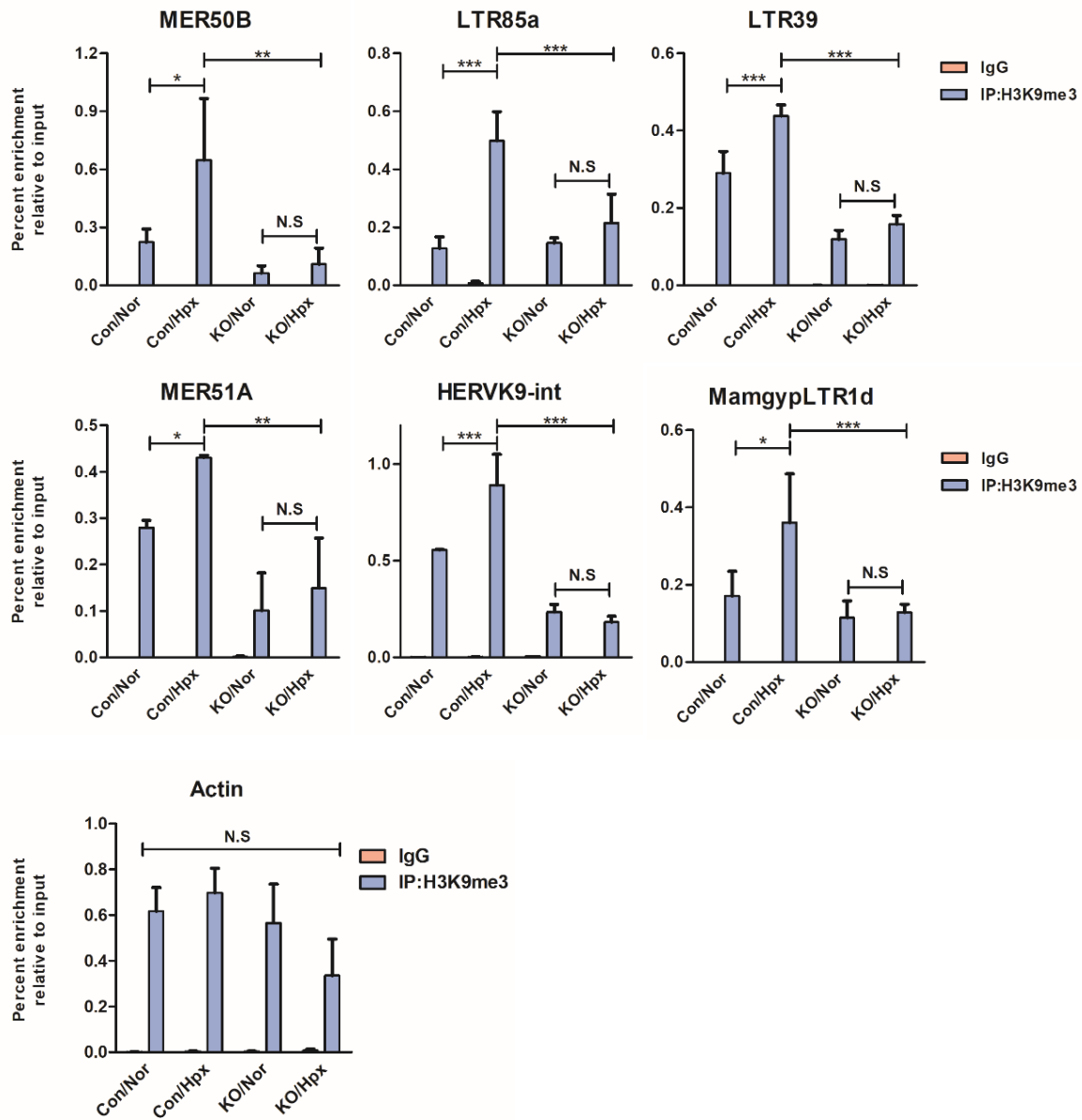
H



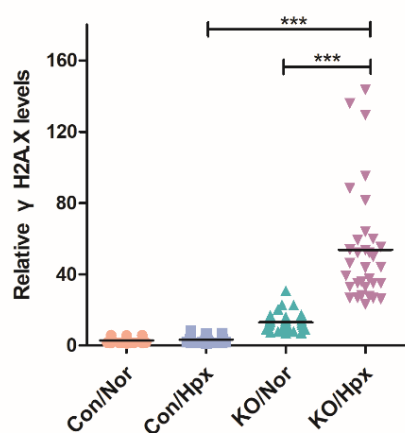
C

D

Fig S7.



J



K

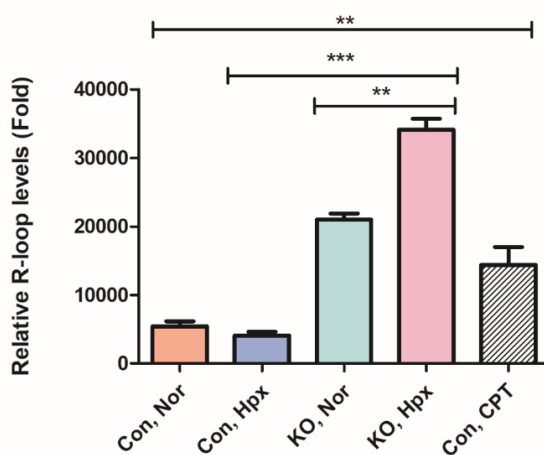
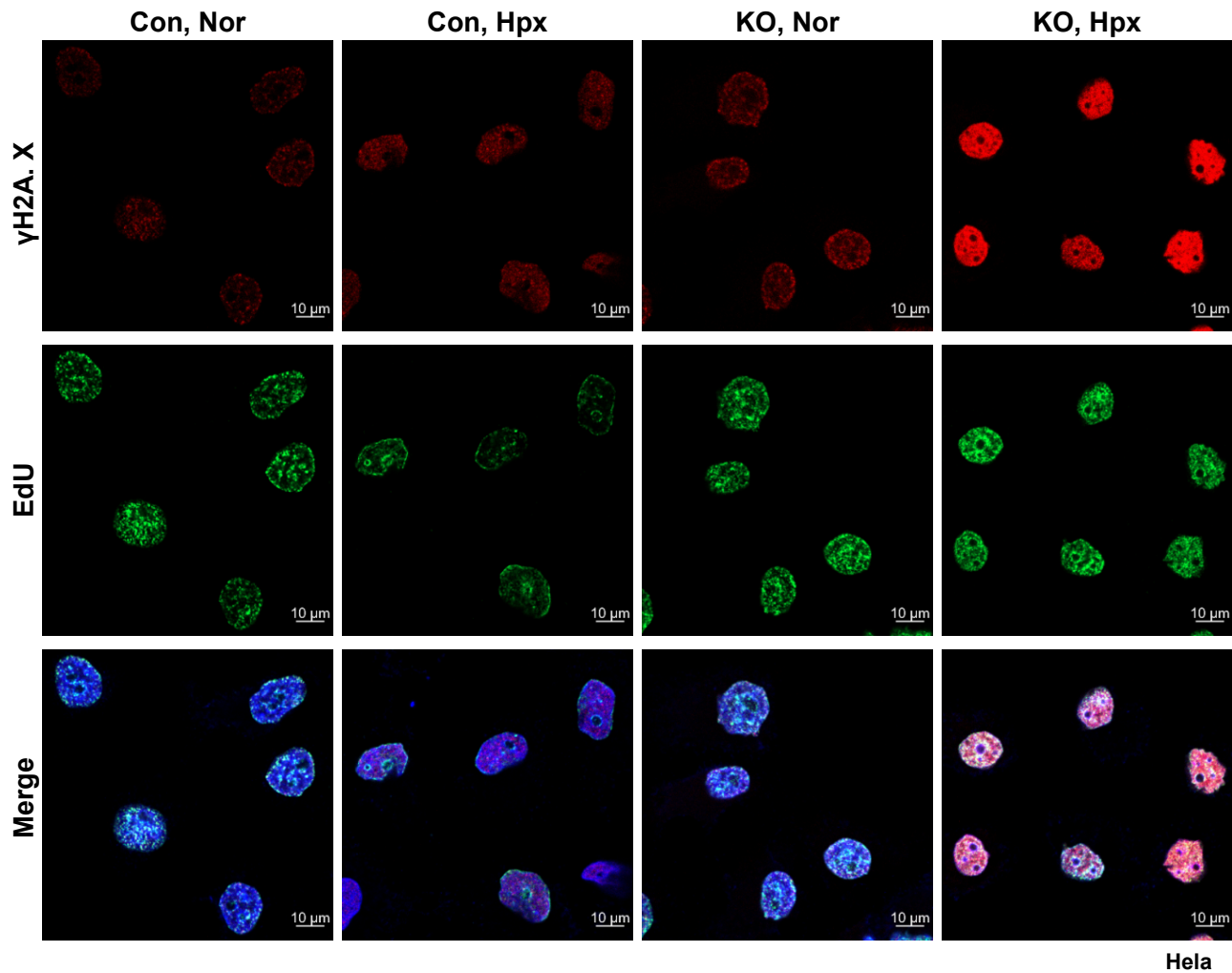
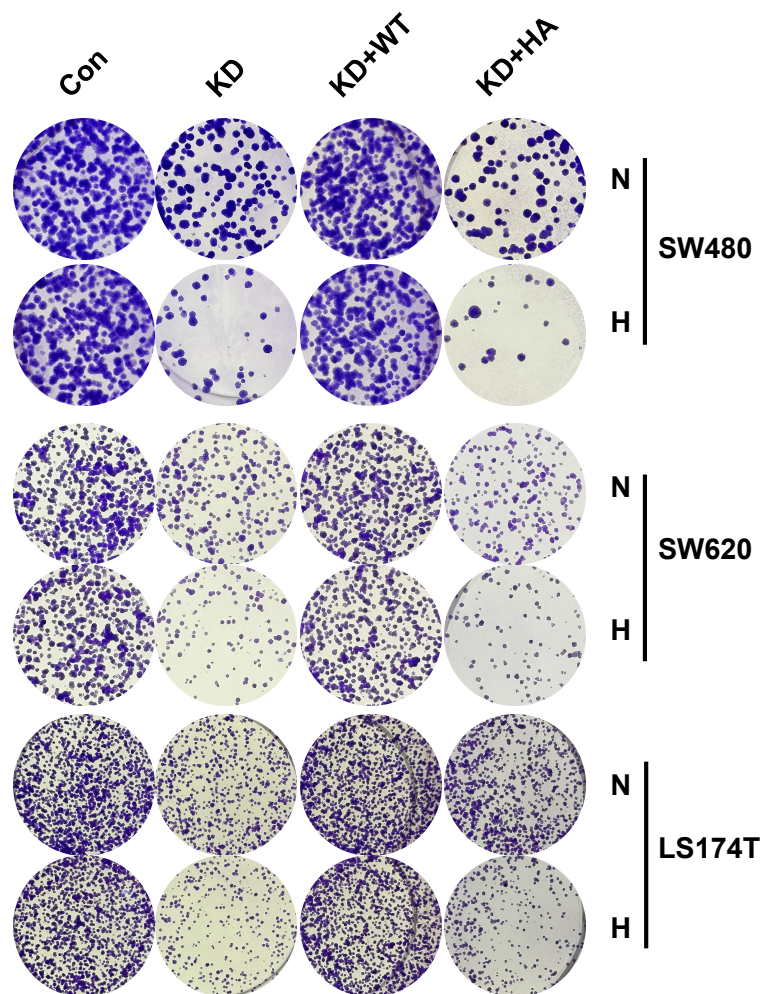


Fig S7.

L



M



N

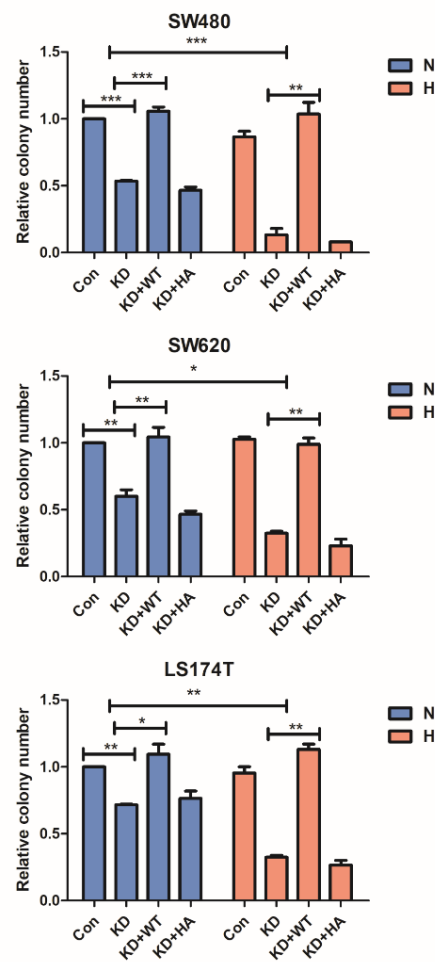
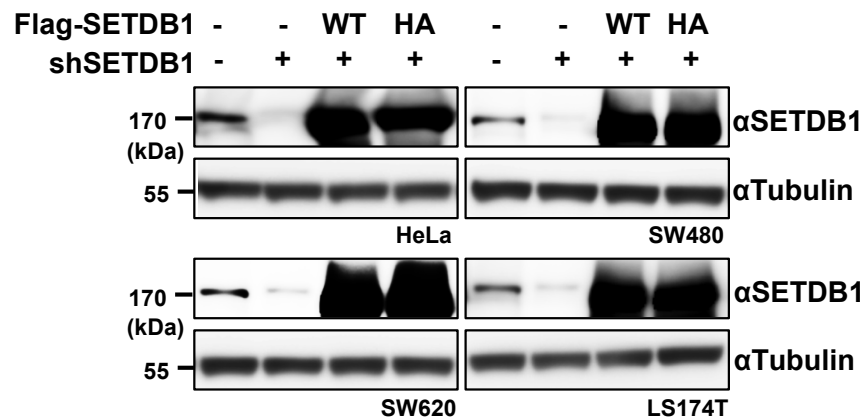
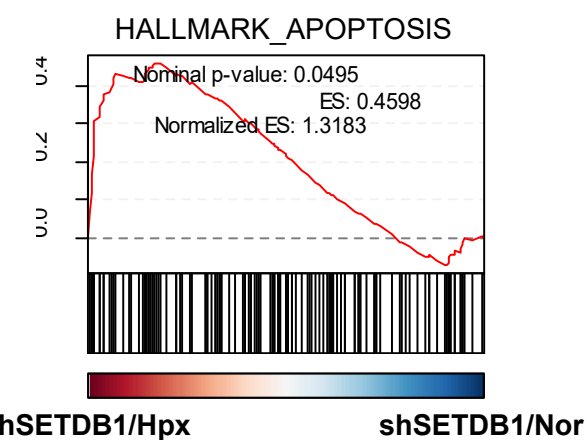


Fig S7.

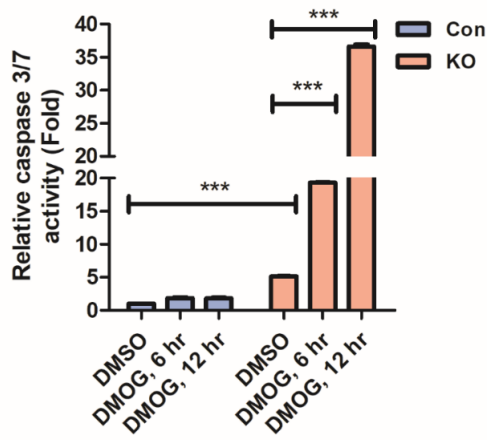
O



P



Q



R

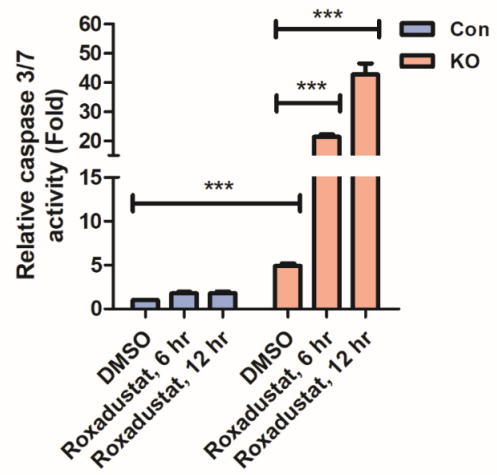
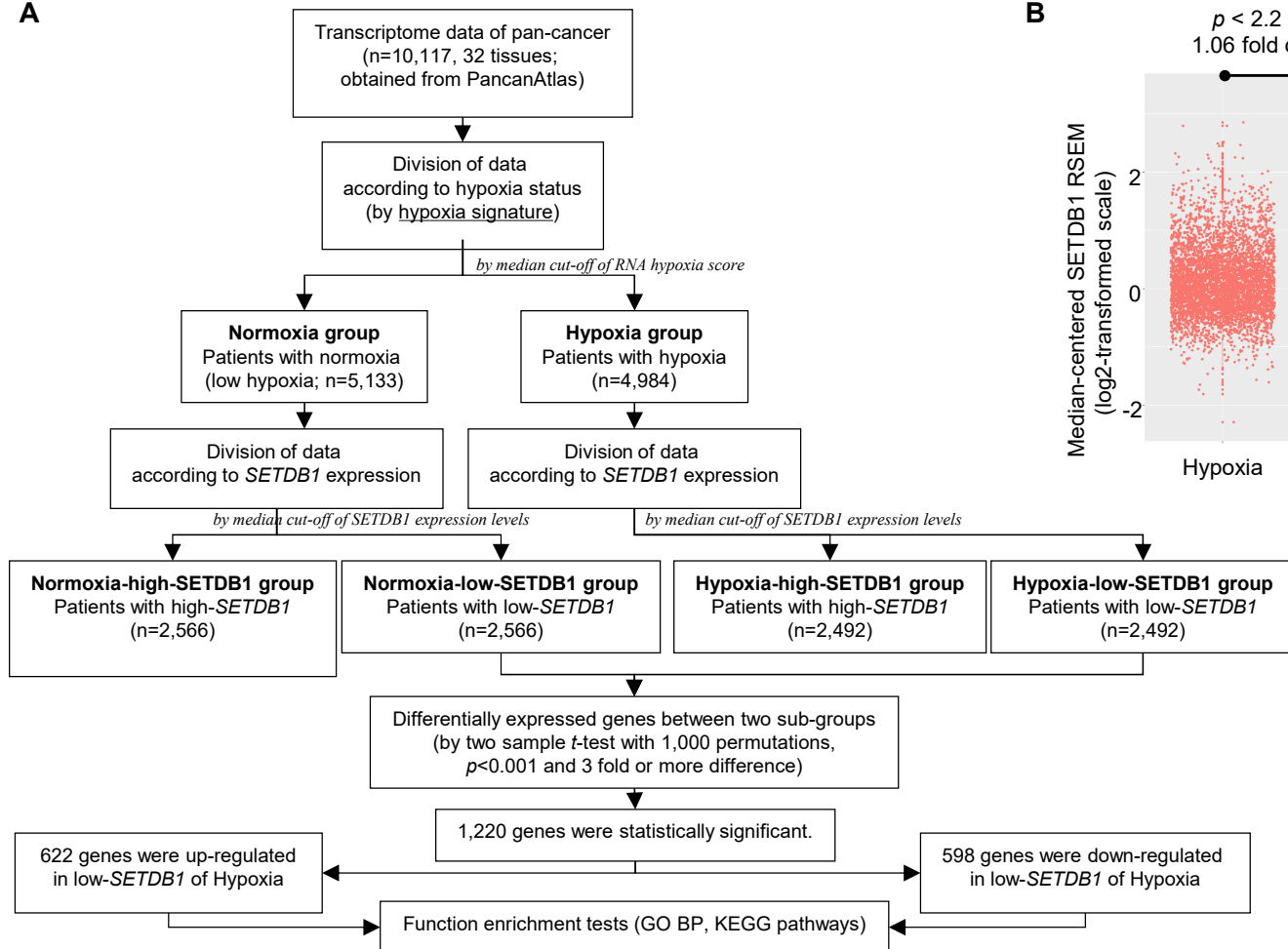


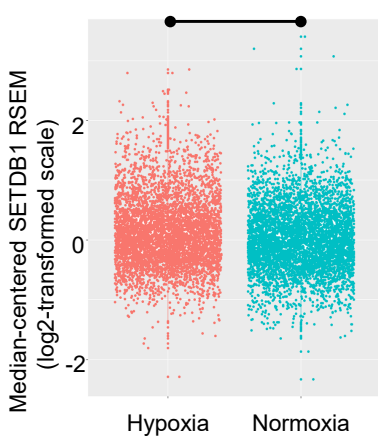
Fig S8.

A

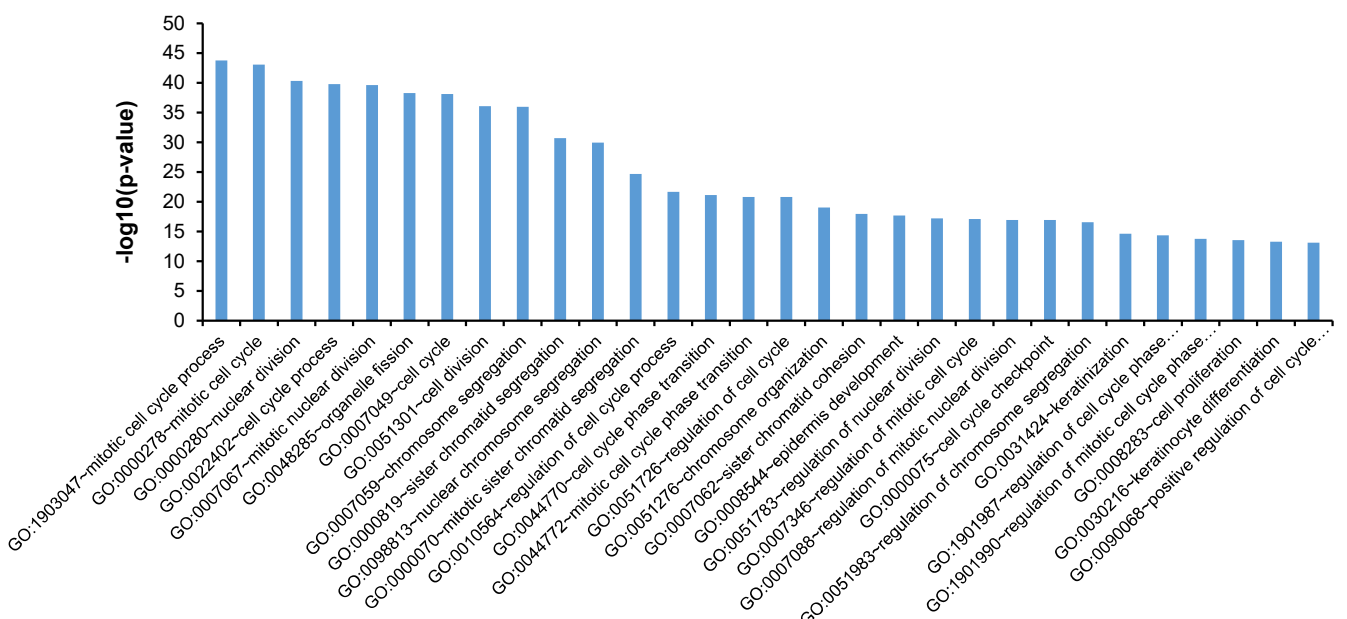


B

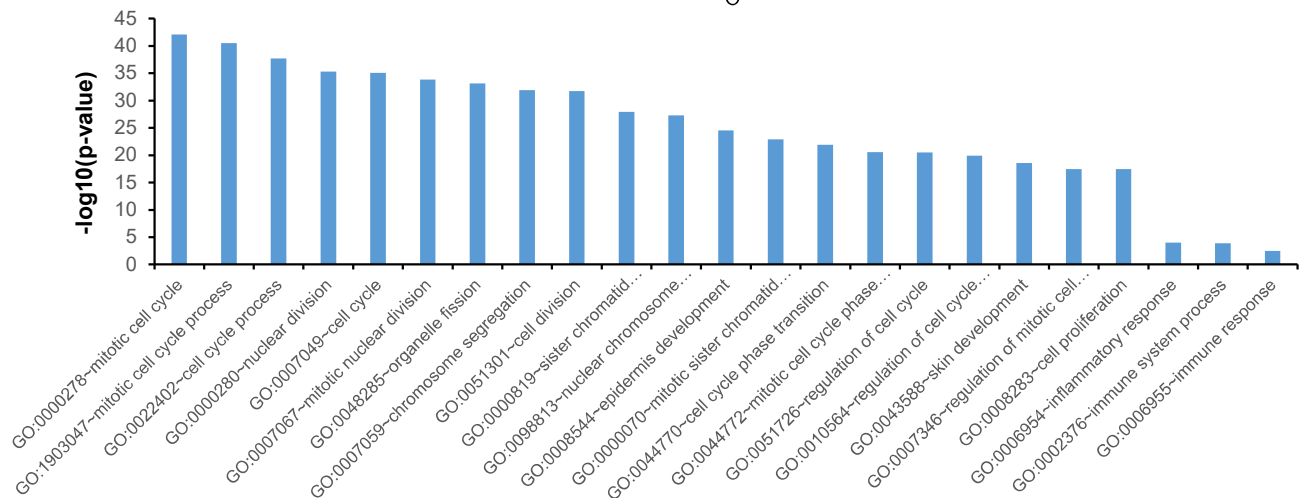
$p < 2.2 \times 10^{-16}$
1.06 fold difference



C



D



Supplementary table S1

A

Cat No.	Antibody	Company	Application
ab107225	SETDB1	Abcam	PLA (1:100)
ab166917	Cullin2	Abcam	WB (1:1000)
ab113077	PHD1	Abcam	WB (1:1000)
ab133630	PHD2	Abcam	WB (1:1000)
ab30782	PHD3	Abcam	WB (1:1000)
ab76493	phospho-IRF3	Abcam	WB (1:1000)
ab109394	phospho-RPA32	Abcam	WB (1:1000)
ab17191	Histone H3	Abcam	WB (1:1000), ChIP
ab8898	H3K9me3	Abcam	WB (1:1000), ChIP
ab290	GFP	Abcam	WB (1:10000), ChIP
ab171870	IgG	Abcam	WB (1:1000), ChIP
A300-169A	ATF7IP (MCAF)	Bethyl Laboratories	WB (1:200)
#2196	SETDB1	CST	IF (1:100)
#68547	VHL	CST	WB (1:1000), ChIP
#2699	cullin4a	CST	WB (1:1000)
#14179	HIF1α	CST	WB (1:1000)
#3724	HA	CST	WB (1:1000)
#5537	HIF1β	CST	WB (1:1000)
#3504	TBK1	CST	WB (1:1000)
#11904	IRF3	CST	WB (1:1000)
#5483	phospho-TBK1	CST	WB (1:1000)
#5321	MDA5	CST	WB (1:1000)
#3743	RIG1	CST	WB (1:1000)
#4764	p65	CST	WB (1:1000)
#3033	phospho-p65	CST	WB (1:1000)
#9718	γH2AX	CST	WB (1:1000)
#13934	ATR	CST	WB (1:1000)
#2873	ATM	CST	WB (1:1000)
#2853	phospho-ATR	CST	WB (1:1000)
#13050	phospho-ATM	CST	WB (1:1000)
#5625	Cleaved PARP	CST	WB (1:1000)
#9761	Cleaved Caspase-3	CST	WB (1:1000)
#9761	Cleaved Caspase-6	CST	WB (1:1000)
#2278	Myc-Tag	CST	WB (1:1000)
#7074S	anti-Rabbit IgG HRP conjugated	CST	WB (1:5000)
#2912	LDHA	CST	WB (1:5000)
#73812	Hydroxyproline	CST	WB (1:1000), IP
NB100-295	PHD4	Novus Biologicals	WB (1:1000)
11231-1-AP	SETDB1	Proteintech	WB (1:1000), ChIP
13536-1-AP	VHL	Proteintech	PLA (1:100)
34650	6X His	QIAGEN	WB (1:1000)
sc-133090	ElonginB	Santa Cruz Biotechnology	WB (1:1000)
sc-135895	ElonginC	Santa Cruz Biotechnology	WB (1:1000)
T5068	Tubulin	Sigma Aldrich	WB (1:1000)
F3165	Flag M2	Sigma Aldrich	WB (1:1000)
F2555	Flag (Rabbit)	Sigma Aldrich	WB (1:1000)
MABE1134	J2	Sigma Aldrich	IF (1:50)
MABE1095	R-loop (DNA-RNA Hybrid)	Sigma Aldrich	IF (1:50)
A11008	bit IgG (H+L) Cross-Adsorbed Secondary Antibody, Alexa	Thermo Fischer	IF (1:1000)
A11010	bit IgG (H+L) Cross-Adsorbed Secondary Antibody, Alexa	Thermo Fischer	IF (1:1000)
A11003	use IgG (H+L) Cross-Adsorbed Secondary Antibody, Alexa	Thermo Fischer	IF (1:1000)
A9044	anti-Mouse IgG HRP conjugated	Sigma-Aldrich	WB (1:5000)

WB; Western blot, IF; Immunofluorescence, PLA; Proximity ligation assay, IP; Immunoprecipitation

B

Application	Gene	Forward (5' - 3')	Reverse (5' - 3')
RT-qPCR	CXCL8	GAGAGTGTATTGAGAGTGGACAC	CACAAACCTCTGCACCCAGTT
RT-qPCR	IL1A	TGTATGTACTCCCCAACATGAAG	AGAGGAGGTTGGCTCACTACC
RT-qPCR	EBI3	TGTTCTCATGGCTCCCTAC	AGAAAGATCTCGGAAAGGCC
RT-qPCR	IL4R	CTGCTCATGGATGACCGTGGTC	GGTGTGACTGTCACTTCTCG
RT-qPCR	GBP2	GTTCCTACATCTCAGCCATTCC	CCACTGCTGATGGCATTGACGT
RT-qPCR	HLA-A	AGATAACCTGCCATGTGCAGC	GATCACAGCTCCAAGGAGAAC
RT-qPCR	RAET1L	AGAGCAACTGCTGACATTAGC	GAGTAGGAAAGGCTGTCATCG
RT-qPCR	LTR39	CCCTTGCTTGTAACTCCCTCA	AAACCTGGGTCTGCTTCCCT
RT-qPCR	HERV9-int	GCAAGCTTGAAGGAATGC	TCAGCACCATGGTCTATC
RT-qPCR	MER51A	ATTAGTCTGCTCCACAAACC	CATAGGGGCTCAAAGCTCAG
RT-qPCR	MER50B	CCACTCTGCTCTGAACACTTG	CATATGGTCTGCAACATC
RT-qPCR	LTR85a	TGGGGAAAGGTGAAGCTTAA	ACTCATTGGGCCATCAGACCC
RT-qPCR	MamGypLTR1d	AATGCCAAACCTGTGTCCTC	TTCTTTCTGGGCCCTCTAT
RT-qPCR	SETDB1	AAAGAGTGTGCCCACAGGG	CATGTTGGTCACAATTGCA
RT-qPCR	Actin	CTCCCTTAATGTCACGCACGAT	CATGTACGTTGCTATCCAGGC
ChIP-qPCR	CXCL8	AGTAGCCCCCTAAAGCAGCT	TGGTGAAGATAAGCCAGCAA
ChIP-qPCR	IL1A	TCTCTATGAGGGCATGGTGA	GAGAACACCAAGGCCACCATCA
ChIP-qPCR	EBI3	AGAGGGTTGTCAAAGGAAGG	ACCCACAAAGTCAGAGGGT
ChIP-qPCR	IL4R	GCCTGCATCCGGGTCTTAA	CACTCTGCAAGGTAACGAGGAG
ChIP-qPCR	ZNF221	AAGGCATGATTTCACCTCA	CTGCTCTTGAATGTGTC
ChIP-qPCR	ZNF37A	CATTCTGAAGAGGAACCTCTG	TTTCTGATGCCAAATGAGGT
ChIP-qPCR	LTR39	AACTCTAGGCCCAACCAAAT	AGCAGGAGGCTCACAGGTAT
ChIP-qPCR	HERV9-int	AGCGGGGATGTTAGGATTAC	TGGCATAATCAGGACTGTG
ChIP-qPCR	MER51A	CCAAATTCAAGCTGACCTCT	GGTTGTGGAGGGGACTAAAT
ChIP-qPCR	MER50B	CTGCTCTGAAACTTGCCTGTC	CCATATGGTCTGCAGCAAT
ChIP-qPCR	LTR85a	AGTGGTCTGTAAGTGA	AAACAGGGTTGTTCTCACG

C

Gene	Target Sequence (5' - 3')
sgSETDB1	GCUCUGAGGACGAUCUCCC
shRNA/siRNA negative control	UUCUCCGAACGUUCAGCU
shSETDB1 (3' UTR)	AUCCCUCCCCAUCCAUUUU
shSETDB1	GCUCAGAUUAACUUCUGUA
shVHL	GGAGGCCAUUGCACAUACG
siMDA5	CCAACAAAAGACGAGGUUA
siRIG1	CCAGAAUUAUCCCAACCGUA
siARNT(HIF1β)	AAUGACAUACAGAUUACCA
siPHD1	AAUGAGCAACCGGUCAAG
siPHD2	UCUGAGUGUAGUAGUACUA
siPHD3	GUUCAGACCCUUACGCAA
siPHD4	CGAUGAAAUGAGUCUGAUU
siVHL #1	GGAGGCCAUUGCACAUACG
siVHL #2	UAUCACACUGCCAGUGUUAAC
siATF7IP	CCCUGUAUCCUAAGUGUUAU

Supplementary table S2

Gene names	Score	Number of Oxidation (P)	Amino acid	Position in peptide	Position in protein	Charge	Sequence window	Oxidation (P) Probabilities
SETDB1	125.53	1	P	11	236	2	KTWIHKGTUAIOTVCPGKKYKVKFDNKGKSL	GTUAIQITVGR(1)GKK
SETDB1	145.52	1,2	P	14	253	3	GKSLSGNHAYDHPADKLIVGSRVVAKY	SLLSGNHIAYDHP(1)R(1)ADE
SETDB1	154.79	1,2	P	15	254	3	KSLSGNHAYDHPADKLIVGSRVVAKY	SLLSGNHIAYDHP(1)R(1)ADE
SETDB1	85.231	1	P	20	312	3	FDDGYASVYTQSELYPICRPLKKTWEDIEDI	FUFFDDGYASVYTQSELYP(1)CCR
SETDB1	123.97	1,2	P	11	341	3	DISCRDFIEEY/TAYPNPRMVLKSGQLIKT	DIEEY/TAYP(1)NRP(1)MVLK
SETDB1	139.08	1,2	P	14	344	3	CRDIEEY/TAYPNPRMVLKSGQLIKT	DIEEY/TAYP(1)NRP(1)MVLK
SETDB1	104.35	1	P	4	430	3	QLRTRPNMGA/RSKGP/VQTQDLTGTTGQF	SKGP(1)VQYTQDLTGTTGQF
SETDB1	314.56	1,2	P	1	496	3	AOQRKQVAKKTSFRPGSVGSHSSPTSPAL	P(1)GSVGSGHSSPTSPALSENVSGGK
SETDB1	223.2	1,2	P	11	506	3	STSFRRPSVVGSHSSPTSPALSENVSGGKPC	PGS/VSCHSSP(1)TSR(1)ALSENVSGGKPCINOTYR
SETDB1	232.2	1,2	P	14	509	3	FRPGSVGSHSSPTSPALSENVSGGKPCINQ	PGS/VSCHSSP(1)TSR(1)ALSENVSGGKPCINOTYR
SETDB1	221.29	1,2,3	P	18	545	3	LGSTASAPASLAPPAPVPHGMLERAPA	SPLGSTASAPASLP(0.005)AP(0.992)AP(0.992)AP(0.01)P(0.001)VFGHMLER
SETDB1	212.32	1,2,3	P	19	546	3	GSTASAPASLAPPAPVPHGMLERAPAEE	SPLGSTASAPASLP(0.005)AP(0.992)P(0.992)AP(0.01)P(0.001)VFGHMLER
SETDB1	215.37	1,2,3	P	21	548	3	TASAPASLAPPAPVPHGMLERAPAEPS	SPLGSTASAPASLP(0.004)P(0.009)AP(0.993)P(0.995)VFGHMLER
SETDB1	235.73	1,2,3	P	22	549	3	ASAPASLAPPAPVPHGMLERAPAEPSY	SPLGSTASAPASLP(0.002)P(0.045)AP(0.955)P(0.998)VFGHMLER
SETDB1	88.224	1	P	5	575	3	AEP/SYRAMEKLFYLHV/CYTCLSRVRPMR	LFYLP(1)HV/CYTCLSR
SETDB1	145.89	1	P	2	599	2	SRVPRMRNEOYRKINPLVPLLYDFRMMTAR	NP(1)LLVPLLYDFR
SETDB1	175.73	1	P	6	603	2	PNRNEOYRKINPLVPLLYDFRMMTARRRN	NPLLUVPI1LLYDFR
SETDB1	131.04	1,2	P	15	755	3	KCACHOLTIQATACTPGQOINPNSGYQYKRL	CACHOLTIQATACTP(1)GGQINP(1)NSGYQYK
SETDB1	136.61	1,2	P	21	761	3	LTIQATACTPGQOINPNSGYQYKRECLECLPT	CACHOLTIQATACTP(1)GGQINP(1)NSGYQYK
SETDB1	114.27	1	P	7	775	3	NPNQSYOYKRLLEECLPTGVYECNKRCKCDPN	RLEECCLP(1)TVG/VECNKR
SETDB1	231.66	1,2	P	6	1065	3	KMSV/TESSRNVGYNPSPV/KPEGLRRPPSKT	NYGYNP(1)SP(1)VKP(1)EGLR
SETDB1	290.28	1,2	P	8	1067	2	SV/TESSRNVGYNPSPV/KPEGLRRPPSKTSM	NYGYNPSP(1)VKP(1)EGLR
SETDB1	322.99	1,2	P	11	1070	2	TESSRNVGYNPSPV/KPEGLRRPPSKTSMHQ	NYGYNPSP(1)VKP(1)EGLR
SETDB1	146.53	1	P	10	1096	3	SM-HOSRLLMASAOSNPDV/LTLSSTESEGE	RLMASALSNP(1)DDVLTLSSTESEGE
SETDB1	188.33	1	P	2	1118	4	SSSTEEGEOEGTSRQPTAGQQTGATAV/DSDDI	KP(1)TACGTSATAV/DSDDQTSGSEGDFFEDKK
SETDB1	159.14	1	P	8	1228	3	KLEGNLGRYLNHSCSPNLVQVNVDTHDLR	YLNHSOSP(1)NLVQVNVDTHDLR
SETDB1	154.49	1	P	2	1245	2	LFVQNVFVDTDLRFPWVAAFKSRIRAGTE	FP(1)WVAFASK

NOTE: Putative hydroxylated proline sites were selected by oxidation (P) probabilities. Sites with probability <1 were excluded.

B

	Normalized hydroxylated proline intensity					
	DMSO			DMOG		
	#1	#2	#2	#1	#2	#3
P575	0.003597588	0.004353763	0.003196034	0.003547332	0.002784024	0.004331632
P599	9.2851E-09	5.58892E-09	3.13108E-09	7.35747E-09	2.07986E-08	1.19756E-09
P603	0.000375119	0.000416592	0.000274284	0.000358129	0.000302209	0.000444416
P755	0.017087195	0.036361209	0.018297891	0.009507979	0.008935644	0.027867333
P761	0.000473913	0.00705437	0.001580862	0.000435378	0.001015277	0.00233271
P775	0.015653739	0.071947001	0.054909034	0.015287595	0.036999564	0.013005681
P1065	0.001442995	0.000195248	0.001786654	0.00168815	0.001044784	0.001410585
P1067	0.002753892	0.002973957	0.002301794	0.001865904	0.002475788	0.003235637
P1070	0.00500171	0.002257816	0.003667044	0.003377893	0.002415626	0.00273898
P1096	0.001269864	0.000824098	0.000229361	0.000600423	0.0003901	0.000228151
P1118	0.002253937	0.00044533	0.001442367	0.00184823	0.001825142	0.002249063
P1228	0.086015477	0.054397885	0.058367013	0.076285516	0.03046268	0.038974617
P1245	0.034207685	0.036566804	0.029713566	0.024914068	0.0222261	0.026693032

Supplementary Figure Legends

Figure S1. Hypoxia stabilizes SETDB1 protein.

(A) Half-life of Flag-SETDB1 protein in shControl (shCon) and shVHL HEK293T cells treated with cycloheximide (50 µg/mL) for the indicated times, determined by immunoblotting with the indicated antibodies. (B) Quantification of results in Figure S1A. (C, D) Effect of siRNA-mediated KD of VHL on polyubiquitination of ectopic Flag-tagged SETDB1 in HEK293T cells treated with bortezomib (1 µM, 12 h), measured by immunoblotting with the indicated antibodies. (E) Upregulation of ubiquitination of overexpressed Flag-tagged SETDB1 by overexpression of Myc-tagged VHL in HEK293T cells treated with bortezomib (1 µM) for 12 h.

Figure S2. Stability of SETDB1 and its binding partner ATF7IP are dependent on oxygen availability.

(A) Inverse correlation of SETDB1 protein expression and oxygen concentration in HEK293T and HeLa cells exposed to different O₂ levels for 3 h, determined by immunoblotting with the indicated antibodies. (B) Quantification of SETDB1 immunofluorescent signals in cells examined for Figure 2B (n > 40, *** p-value < 0.001, Student's t-test). (C) SETDB1 mRNA levels in HeLa cells under normoxia or hypoxia (1% O₂) for the indicated times measured via qRT-PCR. Relative levels were calculated by normalizing to actin mRNA. (D) Immunoblot analysis of SETDB1 and ATF7IP in HeLa cells treated with 2,2-bipyridyl (200 µM) for the indicated times. (E)

SETDB1 protein levels in HeLa cells exposed to different hypoxic conditions. Cells exposed to hypoxic conditions (1% O₂, 3 or 6 h) were rescued under normoxic conditions (Re-O₂) for the indicated times and SETDB1 levels were assessed by immunoblotting. (F) Immunoblot analysis of nuclear SETDB1 levels in HeLa cells with siRNA-mediated knockdown of ATF7IP (siATF7IP) under normoxia or hypoxia (1% O₂, 6 h).

Figure S3. Hypoxia-induced SETDB1 stabilization in different cell lines.

(A) Immunoblot analysis of SETDB1 protein levels in HDFn and HEKa cells under hypoxia. (B-G) Immunoblot analysis of SETDB1 protein levels in cancer cell lines under hypoxia (1% O₂ for the indicated times) or hypoxia mimetic conditions (200 μM 2,2-bipyridyl) for the indicated times. (H) Immunoblot analysis of SETDB1 protein levels in HeLa cells under hypoxic stress (1% O₂, 6 h) or with DMOG (1 mM) or roxadustat (100 μM, 6 h) treatment. (I) Immunoblot analysis of SETDB1 protein levels in RCC4 cells treated with DMOG (1 mM) for the indicated times. (J) SETDB1 protein levels in different cell cycle phase, determined by immunoblot analysis of lysates of cells released from nocodazole (100 ng/ml) arrest in the presence of DMOG (1 mM) or DMSO control. (K) mRNA levels of PHDs in Figure 2G, measured by qRT-PCR. Relative levels were calculated by normalizing to actin mRNA. (L) Additive effect of simultaneous depletion of PHD1-4 on SETDB1 levels in HeLa cells, determined by immunoblotting using the indicated antibodies. Non-targeting siRNA was used as a negative control.

Figure S4. Physical interactions of SETDB1 with PHDs.

(A-D) Analysis of physical interactions of SETDB1 and overexpressed PHD1-4. Endogenous SETDB1 and overexpressed Flag-PHD1 (A), GFP-PHD2 (B), Flag-PHD3 (C), and Flag-PHD4 (D) were immunoprecipitated using the indicated antibodies, followed by immunoblotting.

Figure S5. VHL recognizes hydroxylated proline residues on SETDB1.

(A) Hydroxylation at proline residues on Flag-tagged SETDB1 and HA tagged HIF1 α examined via an *in vitro* hydroxylation assay utilizing recombinant PHD1 and PHD3 (PHDs), followed by immunoblotting with the indicated antibodies. (B) Hydroxylated proline residues of HIF1 α in HEK293T cells with the indicated with DMOG (1 mM) treatment, captured by immunoprecipitation followed by immunoblotting with the indicated antibodies. (C) Flag-tagged, hydroxylated proline-containing SETDB1 in HEK293T cells treated with DMOG (1 mM, 12 h) or 2,2-bipyridyl (200 μ M, 12 h), or exposed to hypoxia (1% O $_2$, 12 h), captured by immunoprecipitation with an anti-OH antibody or anti-Flag antibody followed by immunoblotting with the indicated antibodies. (D) Schematic imaging of SETDB1 truncation mutants. (E) Physical interactions between HA-VHL and T1, T2, or T3 mutant SETDB1 in HEK293T cells determined via immunoprecipitation using an anti-Flag antibody followed by immunoblotting with the indicated antibodies. (F) Physical interactions between HA-VHL and T4, T5, or T6 mutant SETDB1 in HEK293T cells determined via immunoprecipitation using anti-Flag antibody followed by immunoblotting with the

indicated antibodies. (G) VHL-binding, hydroxylated proline residues of SETDB1, identified by mass spectrometry. The intensity of each hydroxylated proline of SETDB1 was calculated by normalizing the indicated hydroxylated proline residue-containing peptide to that of total peptides from SETDB1. (H) Mass spectra of the indicated non-hydroxylated and hydroxylated prolines in SETDB1. (I-L) Physical interactions between diverse mutant SETDB1 (P575A, P755A, P775, P1228A, or P1245A) and HA-VHL in HEK293T cells determined by immunoprecipitation using anti-Flag antibody followed by immunoblotting with the indicated antibodies. (M) Half-lives of wild-type (WT) and mutant SETDB1 with 3PA (3PA) in HEK293T treated with cycloheximide (CHX, 50 µg/ml) for the indicated times analyzed by immunoblotting with the indicated antibodies. (N) Quantitative analysis of half-lives of WT and 3PA SETDB1 proteins. Data are expressed as means ± SD of three independent experiments (* *p*-value < 0.05, Student's t-test). (O) Effect of DMOG (1 mM) treatment on the histone H3K9 methylation activity of Flag-tagged SETDB1, assessed by *in vitro* methylation assay using recombinant core histone (1.5 µg) followed by immunoblotting with the indicated antibodies. (P) Effects of the 3PA mutation on histone H3K9 methylation activity of Flag-tagged SETDB1 (0.5 µg) examined via an *in vitro* methylation assay utilizing recombinant core histone (1.5 µg) followed by immunoblotting with the indicated antibodies.

Figure S6. Immune-inflammatory response is overrepresented in SETDB1 knockout cells in hypoxia.

(A) Multidimensional scaling (MDS) plot of RNA-seq data from HeLa cells depleted of

SETDB1 (shSETDB1) under hypoxic (hpx) versus normoxic (nor) conditions, and in control HeLa cells (shControl) under hypoxic versus normoxic conditions. Each point represents 1 sample. (B) Gene ontology (GO) over-representation in differentially upregulated genes in SETDB1 knockout (KO) HeLa cells under hypoxia compared with control cells under normoxia. Immune-inflammatory response-related GO are presented in orange. (C) Venn diagram displaying gene ontology-biological pathways (GO_BP) identified with gene set enrichment analysis (GSEA). Pathways enriched in HeLa cells depleted of SETDB1 under hypoxia compared with those under normoxia are presented in red. Pathways enriched in control HeLa cells under hypoxia compared with those under normoxia are presented in black. (D) Heatmap showing relative expression of differentially upregulated innate immune signature-related genes in SETDB1 knockout (KO) cells under hypoxia.

Figure S7. Hyperactivated innate-inflammatory response in SETDB1 knockout cells under hypoxia is dependent on derepression of a subset of TEs.

(A) Occupancy of SETDB1 at promoters of different inflammatory response genes and known SETDB1-associated loci (ZNF221 and ZNF37A) analyzed using ChIP-qPCR. (B) Quantification of anti-J2 signal intensity as described in Figure 5A (* p -value < 0.05, ** p -value < 0.005, Student's t-test). (C) Inflammatory signaling activities in RIG1-depleted (siRIG1) cells determined via immunoblot with the indicated antibodies. KO: SETDB1 KO, Con: control. (D) Schematic diagram of analysis of transcripts derived from transposable elements (TE) in KO cells under normoxia (Nor) and hypoxia (Hpx). RE: repetitive element, DETup: differentially upregulated TEs (red), DETdn:

differentially downregulated TEs (blue). (E) Volcano plots displaying \log_2 fold change of TEs in KO/Nor and KO/Hpx compared with those in Con/Nor. (F) Venn diagram of DETs identified in KO/Nor and KO/Hpx compared with those in Con/Nor ($p<0.05$). (G) Heatmap displaying relative expression of DETdns in KO/Nor (C) and KO/Hpx (D). (H) Cumulative distribution of fold changes in transcript abundance for TE groups C and D in SETDB1 KO cells under normoxia (KO/Nor) and hypoxia (1% O₂, 12 h; KO/Hpx) compared with those in control cells under normoxia (Con/Nor). The *p*-values were calculated with the Kolmogorov Smirnov (KS) test. (I) ChIP-qPCR analysis of H3K9me3 enrichment at the indicated TE and Actin loci in SETDB1 KO (KO) and control (Con) HeLa cells under either normoxia or hypoxia (1% O₂, 6 h). Results are expressed as fold enrichment relative to input DNA and presented as mean \pm SEM ($n = 3$, ** *p*-value < 0.005, *** *p*-value < 0.001, Student's t-test). (J) Quantified γ H2AX signal intensities assessed as for Figure 6A ($n>30$, *** *p*-value < 0.001, Student's t-test). (K) Quantification of relative R-loop intensity as described in Figure 6C (* *p*-value < 0.05, ** *p*-value < 0.01, *** *p*-value < 0.001, Student's t-test). (L) Representative immunofluorescent images of anti- γ H2A antibodies (red), EdU (green), and DAPI (blue) in KO and Con cells under normoxia and hypoxia (1% O₂, 24 h). (M) Colony formation assay (CFA) in SETDB1-depleted (KD), control (Con), Wild-type (WT) SETDB1-rescued (Flag-SETDB1 overexpressing) and catalytic dead H1224A (HA) SETDB1-reintroduced colon cancer cells exposed to hypoxia mimetic condition (2,2-bipyridyl, 200 μ M for 24 h) followed by normoxic culture (medium change) for 24 d. N: normoxic condition; H: hypoxia mimetic condition. (N) Quantification of relative colony number as described in Figure S7M (* *p*-value < 0.05, ** *p*-value < 0.01, *** *p*-value < 0.001, Student's t-test). (O) Western blot analysis of knockdown of SETDB1 and re-introduction of wildtype (WT) and catalytic dead H1224A mutant (HA) SETDB1 (Flag-

SETDB1 overexpressing) in SW480, SW620 and LS174T colon cancer cells using the indicated antibodies. (P) GSEA displaying overrepresentation of the ‘hallmark_apoptosis’ pathway in SETDB1-depleted (shSETDB1) HeLa cells under hypoxia compared with shSETDB1 under normoxia. (Q, R) Caspase 3/7 activity in SETDB1-KO (KO) and control HeLa cells exposed to DMOG (1 mM) or roxadustat (100 µM) for the indicated times, assessed with a Caspase-Glo 3/7 Assay.

Figure S8. Transcriptomic profiling of pan-cancer patient data

(A) Overview of transcriptomic data of clinical samples. (B) Expression of the SETDB1 transcript in clinical samples harboring hypoxia and normoxia signatures. (C) Overview of GO pathways overrepresented in the Hypoxia group relative to the Normoxia group. (D) Overview of GO pathways in the Hypoxia-low-SETDB1 group compared with the Normoxia-low-SETDB1 group.

Supplementary table S1.

(A) List of antibodies used in the study. (B) Sequence of primers used for RT-PCR studies (C) Target sequences of siRNA oligonucleotides.

Supplementary table S2.

(A) List of hydroxylated proline containing peptides in SETDB1 identified from LC-MS analysis. (B) Normalized intensity of hydroxylated proline residues on SETDB1 with DMOG (1 mM, 6 h) or DMSO control. Relative insensities were calculated by

normalizing to that of total peptides from SETDB1.